

World Journal of *Clinical Cases*

World J Clin Cases 2021 October 16; 9(29): 8627-8952



REVIEW

- 8627 Time to give up traditional methods for the management of gastrointestinal neuroendocrine tumours
Yozgat A, Kekilli M, Altay M

MINIREVIEWS

- 8647 Healthcare practice strategies for integrating personalized medicine: Management of COVID-19
Liu WY, Chien CW, Tung TH
- 8658 Clinical application of repetitive transcranial magnetic stimulation for post-traumatic stress disorder: A literature review
Cheng P, Zhou Y, Xu LZ, Chen YF, Hu RL, Zou YL, Li ZX, Zhang L, Shun Q, Yu X, Li LJ, Li WH
- 8666 Pros and cons of continuous glucose monitoring in the intensive care unit
Sun MT, Li IC, Lin WS, Lin GM

ORIGINAL ARTICLE**Clinical and Translational Research**

- 8671 Prognostic implications of ferroptosis-associated gene signature in colon adenocarcinoma
Miao YD, Kou ZY, Wang JT, Mi DH

Retrospective Study

- 8694 Cefoperazone sodium/sulbactam sodium *vs* piperacillin sodium/tazobactam sodium for treatment of respiratory tract infection in elderly patients
Wang XX, Ma CT, Jiang YX, Ge YJ, Liu FY, Xu WG
- 8702 Modified Gant procedure for treatment of internal rectal prolapse in elderly women
Xu PP, Su YH, Zhang Y, Lu T
- 8710 Clinical and imaging features of desmoid tumors of the extremities
Shi Z, Zhao XM, Jiang JM, Li M, Xie LZ
- 8718 Retrospective analysis of surgically treated pT4b gastric cancer with pancreatic head invasion
Jin P, Liu H, Ma FH, Ma S, Li Y, Xiong JP, Kang WZ, Hu HT, Tian YT
- 8729 Development of a random forest model for hypotension prediction after anesthesia induction for cardiac surgery
Li XF, Huang YZ, Tang JY, Li RC, Wang XQ

Clinical Trials Study

- 8740** Effects of mindful breathing combined with sleep-inducing exercises in patients with insomnia
Su H, Xiao L, Ren Y, Xie H, Sun XH

Observational Study

- 8749** Chronic hepatitis-C infection in COVID-19 patients is associated with in-hospital mortality
Ronderos D, Omar AMS, Abbas H, Makker J, Baiomi A, Sun H, Mantri N, Choi Y, Fortuzi K, Shin D, Patel H, Chilimuri S
- 8763** Midazolam dose is associated with recurrence of paradoxical reactions during endoscopy
Jin EH, Song JH, Lee J, Bae JH, Chung SJ

CASE REPORT

- 8773** Isolated mass-forming IgG4-related sclerosing cholangitis masquerading as extrahepatic cholangiocarcinoma: A case report
Song S, Jo S
- 8782** *Samonella typhi* infection-related appendicitis: A case report
Zheng BH, Hao WM, Lin HC, Shang GG, Liu H, Ni XJ
- 8789** ACTA2 mutation is responsible for multisystemic smooth muscle dysfunction syndrome with seizures: A case report and review of literature
Yang WX, Zhang HH, Hu JN, Zhao L, Li YY, Shao XL
- 8797** Whole-genome amplification/preimplantation genetic testing for propionic acidemia of successful pregnancy in an obligate carrier Mexican couple: A case report
Neumann A, Alcantara-Ortigoza MA, González-del Angel A, Zarate Díaz NA, Santana JS, Porchia LM, López-Bayghen E
- 8804** Is mannitol combined with furosemide a new treatment for refractory lymphedema? A case report
Kim HS, Lee JY, Jung JW, Lee KH, Kim MJ, Park SB
- 8812** Successful treatment of floating splenic volvulus: Two case reports and a literature review
Sun C, Li SL
- 8820** Removal of "ruptured" pulmonary artery infusion port catheter by pigtail catheter combined with gooseneck trap: A case report
Chen GQ, Wu Y, Zhao KF, Shi RS
- 8825** Isolated neutropenia caused by copper deficiency due to jejunal feeding and excessive zinc intake: A case report
Ohmori H, Kodama H, Takemoto M, Yamasaki M, Matsumoto T, Kumode M, Miyachi T, Sumimoto R
- 8831** Diagnosis and treatment of eosinophilic fasciitis: Report of two cases
Song Y, Zhang N, Yu Y
- 8839** Familial left cervical neurofibromatosis 1 with scoliosis: A case report
Mu X, Zhang HY, Shen YH, Yang HY

- 8846** Successful treatment after toxic epidermal necrolysis induced by AZD-9291 in a patient with non-small cell lung cancer: A case report
Li W, He X, Liu H, Zhu J, Zhang HM
- 8852** Anesthesia management in a pediatric patient with Becker muscular dystrophy undergoing laparoscopic surgery: A case report
Peng L, Wei W
- 8858** Diagnosis of upper gastrointestinal perforation complicated with fistula formation and subphrenic abscess by contrast-enhanced ultrasound: A case report
Qiu TT, Fu R, Luo Y, Ling WW
- 8864** Adenomyoepithelioma of the breast with malignant transformation and repeated local recurrence: A case report
Oda G, Nakagawa T, Mori M, Fujioka T, Onishi I
- 8871** Primary intracranial synovial sarcoma with hemorrhage: A case report
Wang YY, Li ML, Zhang ZY, Ding JW, Xiao LF, Li WC, Wang L, Sun T
- 8879** Lumbar infection caused by *Mycobacterium paragordoniae*: A case report
Tan YZ, Yuan T, Tan L, Tian YQ, Long YZ
- 8888** Primary intratracheal neurilemmoma in a 10-year-old girl: A case report
Wu L, Sha MC, Wu XL, Bi J, Chen ZM, Wang YS
- 8894** Ovarian pregnancy rupture following ovulation induction and intrauterine insemination: A case report
Wu B, Li K, Chen XF, Zhang J, Wang J, Xiang Y, Zhou HG
- 8901** Delayed diagnosis of imperforate hymen with huge hematocolpometra: A case report
Jang E, So KA, Kim B, Lee AJ, Kim NR, Yang EJ, Shim SH, Lee SJ, Kim TJ
- 8906** Acute pancreatitis with hypercalcemia caused by primary hyperparathyroidism associated with paraneoplastic syndrome: A case report and review of literature
Yang L, Lin Y, Zhang XQ, Liu B, Wang JY
- 8915** Use of a modified tracheal tube in a child with traumatic bronchial rupture: A case report and review of literature
Fan QM, Yang WG
- 8923** Isolated liver metastasis detected 11 years after the curative resection of rectal cancer: A case report
Yonenaga Y, Yokoyama S
- 8932** Severe bleeding after operation of preauricular fistula: A case report
Tian CH, Chen XJ
- 8938** Secondary aorto-esophageal fistula initially presented with empyema after thoracic aortic stent grafting: A case report
Wang DQ, Liu M, Fan WJ

- 8946** Disruption of sensation-dependent bladder emptying due to bladder overdistension in a complete spinal cord injury: A case report

Yoon JY, Kim DS, Kim GW, Won YH, Park SH, Ko MH, Seo JH

ABOUT COVER

Editorial Board Member of *World Journal of Clinical Cases*, Jjiang-Huei Jeng, DDS, PhD, Professor, School of Dentistry and Department of Dentistry, National Taiwan University Medical College and National Taiwan University Hospital, School of Dentistry, College of Dental Medicine, Kaohsiung Medical University, Taipei 100, Taiwan. jhjeng@ntu.edu.tw

AIMS AND SCOPE

The primary aim of *World Journal of Clinical Cases (WJCC, World J Clin Cases)* is to provide scholars and readers from various fields of clinical medicine with a platform to publish high-quality clinical research articles and communicate their research findings online.

WJCC mainly publishes articles reporting research results and findings obtained in the field of clinical medicine and covering a wide range of topics, including case control studies, retrospective cohort studies, retrospective studies, clinical trials studies, observational studies, prospective studies, randomized controlled trials, randomized clinical trials, systematic reviews, meta-analysis, and case reports.

INDEXING/ABSTRACTING

The *WJCC* is now indexed in Science Citation Index Expanded (also known as SciSearch®), Journal Citation Reports/Science Edition, Scopus, PubMed, and PubMed Central. The 2021 Edition of Journal Citation Reports® cites the 2020 impact factor (IF) for *WJCC* as 1.337; IF without journal self cites: 1.301; 5-year IF: 1.742; Journal Citation Indicator: 0.33; Ranking: 119 among 169 journals in medicine, general and internal; and Quartile category: Q3. The *WJCC*'s CiteScore for 2020 is 0.8 and Scopus CiteScore rank 2020: General Medicine is 493/793.

RESPONSIBLE EDITORS FOR THIS ISSUE

Production Editor: *Jia-Hui Li*; Production Department Director: *Xiang Li*; Editorial Office Director: *Jin-Lei Wang*.

NAME OF JOURNAL

World Journal of Clinical Cases

ISSN

ISSN 2307-8960 (online)

LAUNCH DATE

April 16, 2013

FREQUENCY

Thrice Monthly

EDITORS-IN-CHIEF

Dennis A Bloomfield, Sandro Vento, Bao-Gan Peng

EDITORIAL BOARD MEMBERS

<https://www.wjgnet.com/2307-8960/editorialboard.htm>

PUBLICATION DATE

October 16, 2021

COPYRIGHT

© 2021 Baishideng Publishing Group Inc

INSTRUCTIONS TO AUTHORS

<https://www.wjgnet.com/bpg/gerinfo/204>

GUIDELINES FOR ETHICS DOCUMENTS

<https://www.wjgnet.com/bpg/GerInfo/287>

GUIDELINES FOR NON-NATIVE SPEAKERS OF ENGLISH

<https://www.wjgnet.com/bpg/gerinfo/240>

PUBLICATION ETHICS

<https://www.wjgnet.com/bpg/GerInfo/288>

PUBLICATION MISCONDUCT

<https://www.wjgnet.com/bpg/gerinfo/208>

ARTICLE PROCESSING CHARGE

<https://www.wjgnet.com/bpg/gerinfo/242>

STEPS FOR SUBMITTING MANUSCRIPTS

<https://www.wjgnet.com/bpg/GerInfo/239>

ONLINE SUBMISSION

<https://www.f6publishing.com>

Clinical and Translational Research

Prognostic implications of ferroptosis-associated gene signature in colon adenocarcinoma

Yan-Dong Miao, Zhi-Yong Kou, Jiang-Tao Wang, Deng-Hai Mi

ORCID number: Yan-Dong Miao 0000-0002-1429-8915; Zhi-Yong Kou 0000-0002-7965-9558; Jiang-Tao Wang 0000-0002-1222-164X; Deng-Hai Mi 0000-0002-8643-4496.

Author contributions: Mi DH designed the research; Miao YD and Kou ZY performed the writing, data analysis, and prepared the figures and tables; Wang JT performed the data validation; Miao YD and Kou ZY contributed equally to this work; All authors approved the final manuscript.

Institutional review board

statement: TCGA and GEO belong to public databases. The patients involved in the database have obtained ethical approval. Users can download relevant data for free for research and publish relevant articles. Our study is based on open-source data, so there are no ethical issues and other conflicts of interest.

Therefore, the current research was exempt from approval by the local ethics committee. The present study follows the data access strategy and publication guidelines of the TCGA and GEO databases.

Conflict-of-interest statement: All authors declare having no conflict of interests.

Yan-Dong Miao, Jiang-Tao Wang, Deng-Hai Mi, The First Clinical Medical College, Lanzhou University, Lanzhou 730000, Gansu Province, China

Zhi-Yong Kou, Department of Oncology, The First Affiliated Hospital of Kunming Medical University, Kunming 650000, Yunnan Province, China

Deng-Hai Mi, Dean's Office, Gansu Academy of Traditional Chinese Medicine, Lanzhou 730000, Gansu Province, China

Corresponding author: Deng-Hai Mi, MD, Chief Doctor, Dean, Professor, Dean's office, Gansu Academy of Traditional Chinese Medicine, No. 418 Guazhou Road, Qilihe District, Lanzhou 730000, Gansu Province, China. mi.dh@outlook.com

Abstract**BACKGROUND**

Colon adenocarcinoma (COAD) is one of the most common and fatal malignant tumors, which increases the difficulty of prognostic predictions. Thus, new biomarkers for the diagnosis and prognosis of COAD should be explored. Ferroptosis is a recently identified programmed cell death process that has the characteristics of iron-dependent lipid peroxide accumulation. However, the predictive value of ferroptosis-related genes (FRGs) for COAD still needs to be further clarified.

AIM

To identify some critical FRGs and construct a COAD patient prognostic signature for clinical utilization.

METHODS

The Cancer Genome Atlas database (TCGA) and Gene Expression Omnibus databases were the data sources for mRNA expression and corresponding COAD patient clinical information. Differentially expressed FRGs were recognized using R and Perl software. We constructed a multi-FRG signature of the TCGA-COAD cohort by performing a univariate Cox regression and least absolute shrinkage and selection operator Cox regression analysis. COAD patients from the Gene Expression Omnibus cohort were utilized for verification.

RESULTS

Our research showed that most of the FRGs (85%) were differentially expressed

Data sharing statement:

Bioinformatics analysis code and dataset available from the corresponding author at mi.dh@outlook.com.

Open-Access: This article is an open-access article that was selected by an in-house editor and fully peer-reviewed by external reviewers. It is distributed in accordance with the Creative Commons Attribution NonCommercial (CC BY-NC 4.0) license, which permits others to distribute, remix, adapt, build upon this work non-commercially, and license their derivative works on different terms, provided the original work is properly cited and the use is non-commercial. See: <http://creativecommons.org/licenses/by-nc/4.0/>

Manuscript source: Invited manuscript

Specialty type: Oncology

Country/Territory of origin: China

Peer-review report's scientific quality classification

Grade A (Excellent): 0
Grade B (Very good): B
Grade C (Good): 0
Grade D (Fair): 0
Grade E (Poor): 0

Received: March 25, 2021

Peer-review started: March 25, 2021

First decision: June 14, 2021

Revised: June 17, 2021

Accepted: August 19, 2021

Article in press: August 19, 2021

Published online: October 16, 2021

P-Reviewer: Abdellateif MS

S-Editor: Wang LL

L-Editor: Filipodia

P-Editor: Liu JH



between the corresponding adjacent normal tissues and cancer tissues in the TCGA-COAD cohort. Seven FRGs were related to overall survival (OS) in the univariate Cox analysis (all $P < 0.05$). A model with five FRGs (*AKR1C1*, *AKR1C3*, *ALOX12*, *CRYAB*, and *FDFT1*) was constructed to divide patients into high- and low-risk groups. The OS of patients in the high-risk group was significantly lower than that of the low-risk group (all $P < 0.01$ in the TCGA and Gene Expression Omnibus cohorts). The risk score was an independent prognosticator of OS in the multivariate Cox analysis (hazard ratio > 1 , $P < 0.01$). The predictive capacity of the model was verified by a receiver operating characteristic curve analysis. In addition, a nomogram based on the expression of five hub FRGs and risk score can precisely predict the OS of individual COAD cancer patients. Immune correlation analysis and functional enrichment analysis results revealed that immunology-related pathways were abundant, and the immune states of the high-risk group and the low-risk group were different.

CONCLUSION

In conclusion, a novel five FRG model can be utilized for predicting prognosis in COAD. Targeting ferroptosis may be a treatment option for COAD.

Key Words: Colon adenocarcinoma; Ferroptosis; Immune status; Prognosis; Overall survival

©The Author(s) 2021. Published by Baishideng Publishing Group Inc. All rights reserved.

Core Tip: Colon adenocarcinoma is one of the most ordinary and fatal malignant tumors. Ferroptosis is a recently appeared type of programmed cell death process, which has the characteristics of iron-dependent lipid peroxide accumulation. In this work, we excavated five ferroptosis-related genes of colon adenocarcinoma from The Cancer Genome Atlas database. Then, we constructed a very accurate prognostic model based on the five genes (*AKR1C1*, *AKR1C3*, *ALOX12*, *CRYAB*, *FDFT1*). Our study also highlights the crucial roles of the risk score was an independent prognostic biomarker for colorectal cancer patients, and we validated these genes in the outside data access (GSE39582).

Citation: Miao YD, Kou ZY, Wang JT, Mi DH. Prognostic implications of ferroptosis-associated gene signature in colon adenocarcinoma. *World J Clin Cases* 2021; 9(29): 8671-8693

URL: <https://www.wjgnet.com/2307-8960/full/v9/i29/8671.htm>

DOI: <https://dx.doi.org/10.12998/wjcc.v9.i29.8671>

INTRODUCTION

According to Global Cancer Statistics 2020[1], colon cancer is one of the most fatal cancers, with approximately 1148515 new cases and 576858 deaths from 36 cancers in 185 countries. The incidence and mortality are both ranked fifth worldwide in 2020. It is the fifth most commonly diagnosed cancer in men and the fourth most frequently diagnosed cancer in women. The incidence rates of colon cancer vary by approximately 9-fold in different regions of the world, with the highest rates in Europe, Australia/New Zealand and North America, with Hungary and Norway ranking first for men and women, respectively. The development of colon cancer is a complex biological process caused by a variety of factors, including obesity, lifestyle, eating habits, and environmental influences[2]. A systematic review and meta-analysis of 43 randomized controlled trials or cohorts indicated that dietary fiber led to a reduced risk of colorectal cancer (CRC), while red and preserved meats led to an increased risk and was rated "convincing," which is the strongest grade assigned[3-5]. Despite significant advances in diagnosis and treatment, the average 5-year overall survival (OS) rate for CRC is 48%, and the 5-year OS rate for patients with metastatic colon cancer is only 10%[6,7]. The complex biological factors and high heterogeneity associated with colon cancer increase the difficulty of predicting prognosis. In

addition, given the limited treatment strategies for colon cancer, it is imperative to develop new prognostic models. The application of second-generation DNA sequencing technology by whole-transcriptome, whole-genome, and whole-exome methods can lead to remarkable advances in cancer genomics[8], and the Cancer Genome Atlas (TCGA) has led to unprecedented opportunities for the study of clinically significant cancer biology[9].

In 2012, Dixon first proposed that ferroptosis was a new form of cell death[10]. Unlike apoptosis, autophagy, and necrosis in terms of biochemistry, morphology, and genetics, ferroptosis is a unique reactive oxygen species-reliant and iron-dependent form of nonapoptotic cell death in which cytological changes are the main features [11]. The iron-dependent accumulation of lipid hydroperoxides to lethal levels is characterized by ferroptosis-regulated cell death[12-15]. Previous studies have shown that ferroptosis was originally defined in RAS-mutated cancer cells. Sensitivity to the induction of ferroptosis is mainly found in numerous diverse types of cancer cells with RAS mutations[16,17]. Lanperisone facilitates the production of reactive oxygen species to kill embryonic fibroblasts of K-Ras-mutant mice by ferroptosis methods, and in a mouse model, it induced ferroptotic death in lung cancer cells by inhibiting Cys2 uptake[18]. The induction of ferroptosis has become an encouraging treatment option for inducing cancer cell death, particularly for malignancies resistant to conventional therapies[19-21].

In addition to ferroptosis inducers, many genes have also been identified as markers or modulators of ferroptosis, such as iron metabolism-related genes, including transferrin receptor 1, transferrin, ferritin heavy chain 1, and ferritin light chain[19]. Previous studies have shown that ferroptosis plays an essential role in several cancers and several genes, such as *Nrf2*, which promotes cancer progression by negatively regulating ferroptosis. of tumor suppressor P53 (TP53), as a transcriptional repressor of SLC7A11, participates in ferroptosis, impairs cysteine input, and promotes the initiation of ferroptosis[22-24]. MUC1-C can upregulate the expression of glutathione by forming a complex with CD44v, which can lead to ferroptosis in breast cancer cells [25]. The coinhibition of NFS1 and Cys transport can cause hypertrophy *in vitro* and inhibit lung cancer cell growth[26]. However, whether these ferroptosis-related genes (FRGs) are related to colon adenocarcinoma (COAD) patient prognosis is still largely unknown.

In the current research, we obtained mRNA expression data and corresponding clinical information on COAD patients from two public databases. In addition, we constructed a prognostic model based on five differentially expressed FRGs from the TCGA-COAD cohort and validated it in the Gene Expression Omnibus (GEO)-GSE39582 cohort. Furthermore, we performed an immune correlation analysis and functional enrichment analysis to identify the potential mechanisms.

MATERIALS AND METHODS

Data collection

TCGA-COAD cohort and GSE39582 cohort: We obtained level 3 RNA-sequencing (RNA-seq) information and corresponding clinical data of COAD from the TCGA database (Data Release 27.0, October 29, 2020, <https://tcga-data.nci.nih.gov/tcga/>). Detailed data selection criteria for mRNA sequencing include the following: (1) The keywords for cases were [Primary Site] "colon," [Program] "TCGA," [Project] "TCGA-COAD," and [Disease Type] "Adenomas and Adenocarcinomas;" (2) The keywords for files are [Data Category] "Transcriptome Profiling," [Data Category] "Gene Expression Quantification," [Experimental Strategy] "RNA-Seq," and [Workflow Type] "HTSeq - FPKM;" and (3) The filter criteria of clinical data are [Data Category] "Clinical" and [Data Format] "BCR XML". We obtained 437 mRNA expression profiles for COAD. Among them, 39 (8.9%) samples were normal and 398 samples (91.1%) were cancerous. The data from the GSE39582 cohort were obtained from the GEO database (<https://www.ncbi.nlm.nih.gov/geo/>) and used for verification, and they consisted of 585 samples (<https://www.ncbi.nlm.nih.gov/geo/query/acc.cgi?acc=GSE39582>) that contained 19 colon mucosa samples and 566 stage I-IV colon adenocarcinoma samples. We normalized the raw data of the gene chip by the RMA algorithm provided by the R package "limma"[27]. The patients' clinicopathological features are listed in Table 1. The mRNA expression and clinical data are both available from public databases (TCGA and GEO). Therefore, the current research was exempt from approval by the local ethics committee. The present study follows the data access strategy and publication guidelines of the TCGA and GEO databases.

Table 1 Clinicopathological features of the colon adenocarcinoma patients in two databases, *n* (%)

	TCGA-COAD	GSE39582
Number of patients	385	566
Survival status		
Alive	306 (79.5)	371 (65.5)
Dead	79 (20.5)	191 (33.7)
Unknown		4 (0.8)
Survival time in d		
Range for OS days	0-4502	0-2412
OS days, median	670	612
Age in yr	67.00 ± 12.76	66.87 ± 13.28
Range	31-90	22-97
Median	69	68
Sex		
Female	180 (46.7)	256 (45.2)
Male	205 (53.2)	310 (54.8)
Stage		
I	66 (17.1)	33 (5.8)
II	151 (39.2)	264 (46.6)
III	103 (26.8)	205 (36.2)
IV	54 (14.0)	60 (10.6)

TCGA-COAD: The Cancer Genome Atlas database-colon adenocarcinoma; OS: Overall survival.

Then, 60 FRGs were obtained from the previous literature[12,20,28] and were shown in [Supplementary Table 1](#).

Construction and validation of the prognostic model of FRGs

The Wilcox test in the R package “limma” was utilized to explore the differentially expressed FRGs (DEFGRs) between corresponding adjacent non-neoplastic tissues and cancer tissues in the TCGA-COAD cohort (false discovery rate < 0.05). FRGs with prognostic values for OS were screened out by a univariate Cox analysis ($P < 0.05$). The interacting genes between FRGs with prognostic values and DEFGRs were visualized through the R package “Venn”[29]. The R packages “igraph” and “reshape2” were used to perform the correlation analysis of interacting genes.

To minimize the risk of overfitting, a least absolute shrinkage and selection operator Cox regression analysis[30] was used to construct the optimal model of FRGs using the R-package “glmnet.” The response variables were the status and OS of TCGA-COAD patients, and the independent variable in the regression analysis was the standardized expression data of candidate prognostic DEFGRs. The risk score for each patient was computed based on the normalized expression level of each FRG and their corresponding regression coefficients. The formula was defined as follows: $Risk\ score = \sum_{j=1}^n Coefficient(n) \times gene\ expression(n)$, where $Coefficient(n)$ denotes the coefficient and indicates the relative expression levels of each ferroptosis-associated gene in the prognostic risk score model. The median risk score was chosen as the cut-off value for TCGA-COAD cohort dichotomy, and the COAD patients were categorized into high- and low-risk groups. Survival information was obtained from the clinical data of the aforementioned samples. We used the R packages “survminer” and “survival” to draw the survival curve according to the high- and low-risk values. Based on the expression of ferroptosis-associated genes in the model, a principal component analysis was carried out with the R package “ggplot2” and t-distributed stochastic neighbor embedding was used to identify the distribution of diverse groups using the R package “Rtsne.” Receiver operating characteristic (ROC) curves were utilized to

examine the sensitivity and specificity of survival prediction by the ferroptosis-associated risk score and were drawn using the R package “survival ROC.” The area under the curve (AUC) value is an accurate prognostic indicator. The risk curve, heatmap, and survival state map were drawn according to the diverse risk scores of the patients. The independent prognostic FRGs were identified by univariate and multivariate Cox hazard regression analyses. A total of 566 COAD patient samples with prognostic information from the GSE39582 dataset were used as verification cohorts to validate the predictive ability of the ferroptosis-associated gene prognostic model based on TCGA-COAD data.

Exploitation of a nomogram based on the five essential FRGs

A nomogram was drawn according to the expression of five FRGs by using the R packages “Hmisc,” “Formula,” “lattice,” “foreign,” “rms,” and “ggplot2.” In addition, a calibration curve was utilized to evaluate the consistency between actual and predicted survival rates. Furthermore, the consistency index was computed to evaluate the prognostic capability of the model. Values of 0.5 and 1.0 represent a random probability and an excellent performance for predicting survival with the model, respectively.

Differential gene expression analysis of five hub ferroptosis-associated genes

We applied the “FUNCTIONS-Expression analysis- Expression DIY-Box Plot” component of the webserver: Gene expression profiling interactive analysis[31] (GEPIA2, <http://gepia2.cancer-pku.cn/#analysis>) to acquire box plots of different expression between corresponding normal tissues from the Genotype-tissue expression database and tumor tissues using the following parameters: log2FC (Fold change) cutoff = 2, *P* value cutoff = 0.05, and “Match TCGA normal and Genotype-tissue expression data.” In addition, we acquired a violin illustration of the expression levels of five FRGs in COAD and the corresponding normal tissues of Genotype-tissue expression and TCGA. We drew box and violin plots by using log2 [TPM (transcripts per million) +1] converted expression data.

We used the Human Protein Atlas (<http://www.proteinatlas.org/>) database to explore the expression level of the core FRGs in the normal and tumor samples. For most of the protein-coding genes, we performed an immunohistochemistry analysis according to the tissue microarray analysis of each protein and the corresponding cancer type of patients. Immunohistochemistry staining was conducted based on prior published literature. The staining index scores were distributed as follows: staining intensity (negative: 0; weak: 1; moderate: 2; and strong: 3) and positive staining (0: < 5%; 1: 5-25%; 2: 26-50%; 3: 51-75%; 4: > 75%). The staining index score was computed by multiplying the staining intensity score by the positive staining score, which ranged from 0 to 12[32].

Functional enrichment analysis of FRGs

Based on the DEFRGs between the high- and low-risk groups, we performed Gene Ontology (GO) and Kyoto Encyclopedia of Genes and Genomes (KEGG) pathway analyses using the R packages “clusterProfiler,” “enrichplot,” “org.Hs.eg.db,” and “ggplot2.” Then, we calculated the activity of 13 immune-related pathways and the infiltration score of 16 immune cells *via* a single-sample gene set enrichment analysis using the R packages “GSVA” and “GSEABase.”

Statistical analysis

We compared the differential expression of FRGs between corresponding adjacent nonneoplastic tissues and COAD tissues by the Wilcoxon test. The OS between diverse groups was contradistinguished based on a Kaplan-Meier analysis with the log-rank test. We explored the independent predictors of OS by using univariate and multivariate Cox regression analyses. The Mann-Whitney test with adjusted *P* values through the Benjamini and Hochberg method was used to contradistinguish the single-sample gene set enrichment analysis scores of immune cells or pathways between the high- and low-risk groups. All statistical analyses were performed with R software (Version-4.0.3). *P* < 0.05 indicated statistical significance and all *P* values were two-tailed.

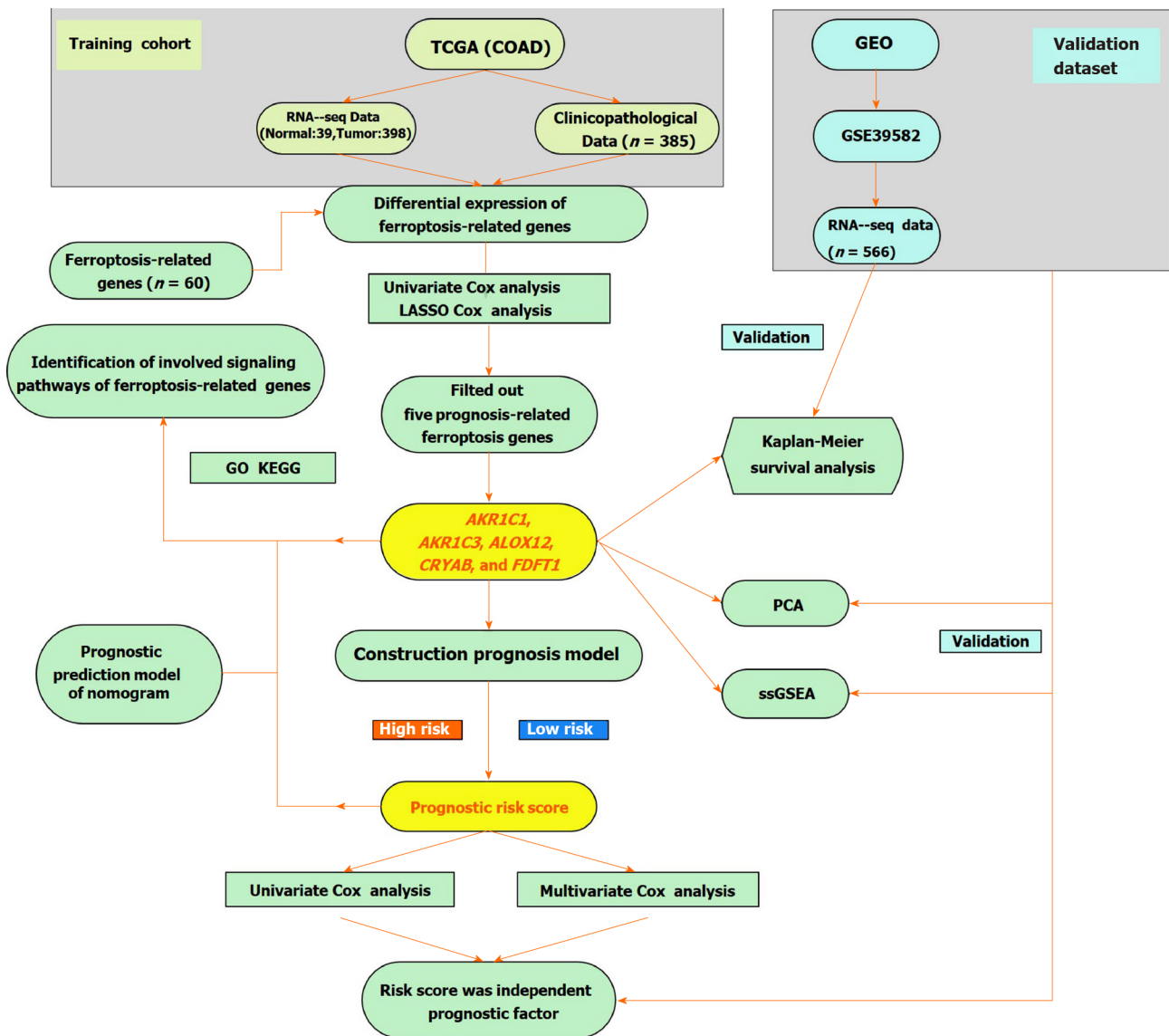


Figure 1 A flow chart of the study design and analysis. TCGA: The Cancer Genome Atlas; COAD: Colon adenocarcinoma; LASSO: Least absolute shrinkage and selection operator; GO: Gene Ontology; KEGG: Kyoto Encyclopedia of Genes and Genomes; ssGSEA: Single-sample gene set enrichment analysis; PCA: Principal component analysis; GEO: Gene Expression Omnibus.

RESULTS

We enrolled 385 COAD patients from the TCGA-COAD cohort and 566 COAD patients from the GEO (GSE39582) dataset. The detailed clinical features of these patients are shown in [Table 1](#). The flow chart of this current study is shown in [Figure 1](#).

Identification of prognostic DEFRGs in the TCGA-COAD cohort

Most of the FRGs (51/60, 85%) were differentially expressed between corresponding adjacent non-neoplastic tissues and COAD tissues, with 31 upregulated FRGs and 20 downregulated FRGs in the COAD tissues ([Figure 2A](#)). A total of seven DEFRGs were related to OS in the univariate Cox regression analysis. *AKR1C3*, *ATP5MC3* and farnesyl-diphosphate farnesyltransferase 1 (*FDFT1*) were low-risk DEFRGs [hazard ratio (HR) < 1, *P* < 0.05]; and *AKR1C1*, *ALOX12*, *CARS1*, and crystallin alpha B (*CRYAB*) were high-risk DEFRGs (HR > 1, *P* < 0.05) ([Figure 2B](#) and [C](#)). The interaction network among these genes demonstrated that *AKR1C1*, *AKR1C3*, *ATP5MC3*, *CARS1*, *CRYAB*, and *FDFT1* are the core genes ([Figure 2D](#)). *ALOX12* positively correlated with *AKR1C1* while negatively correlated with *FDFT1* and *ATP5MC3*. *AKR1C1* has a positive correlation with *ALOX12*, *AKR1C3*, and *CRYAB* while negatively correlated with *FDFT1*. *AKR1C3* positively correlated with *AKR1C1* and *ATP5MC3*. *FDFT1* has a positive correlation with *ATP5MC3* while negatively correlated with *ALOX12*,

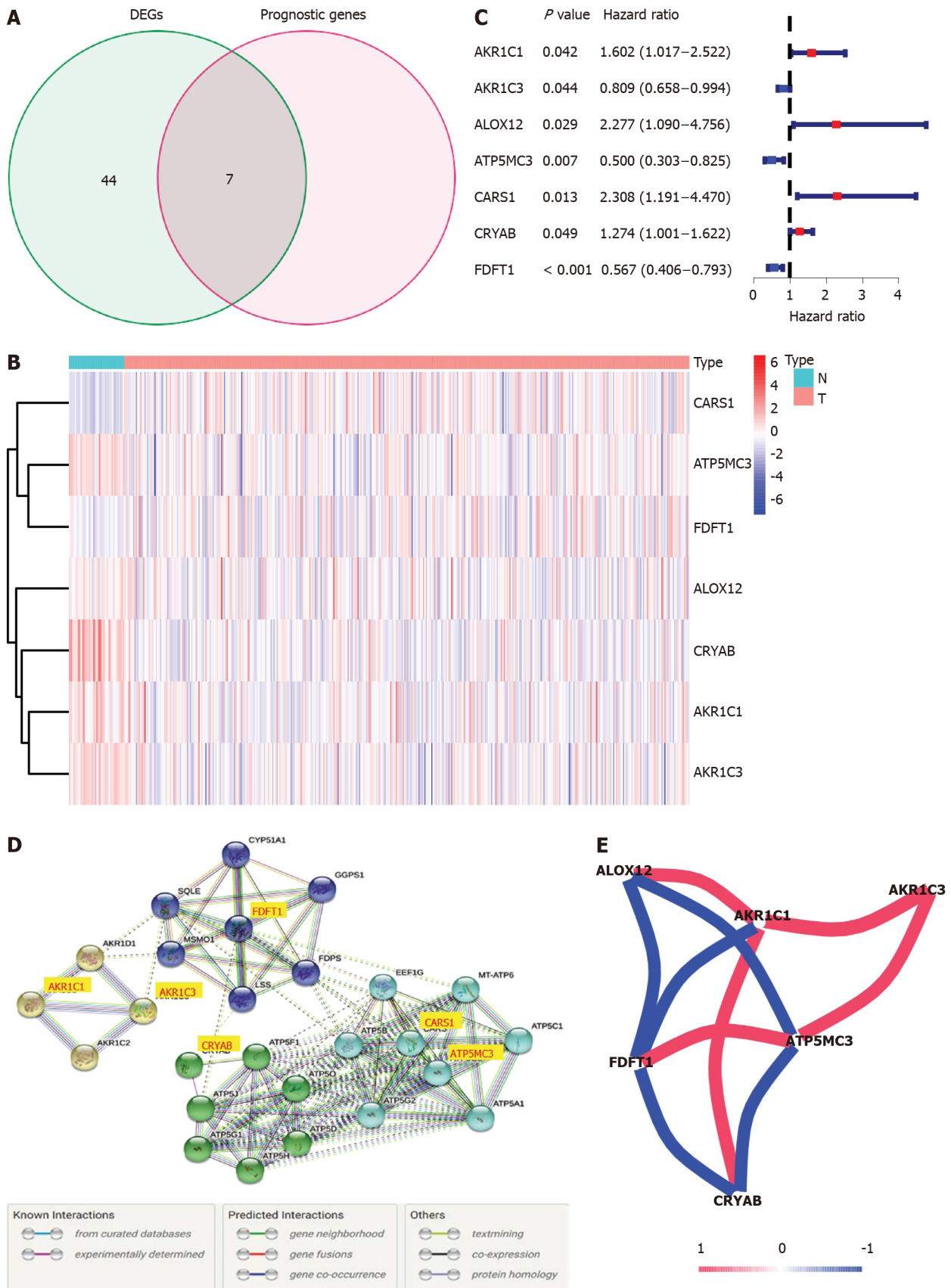


Figure 2 Identification of the candidate prognostic ferroptosis-related genes in the Cancer Genome Atlas-colon adenocarcinoma cohort. A: Venn diagram to confirm differentially expressed genes between corresponding adjacent normal tissue and tumor tissue related to overall survival; B: Heatmap of the seven prognostic ferroptosis-related gene expression profiles in the Cancer Genome Atlas-colon adenocarcinoma cohort; C: Forest plots demonstrated the results of the univariate Cox regression analysis between the expression of the seven prognostic ferroptosis-related genes and overall survival; D: PPI network obtained from the STRING database indicated the interactions among the candidate genes; E: Correlation network of candidate genes. The correlation coefficients are shown using

different colors. DEGs: Differentially expressed genes.

AKR1C1, and *CRYAB*. *ATP5MC3* positively correlated with *AKR1C3* and *FDFT1* while negatively correlated with *ALOX12* and *CRYAB*. The correlation between these genes is shown in [Figure 2E](#).

Construction of a prognostic signature for TCGA-COAD cohort

Five FRGs were screened out by the least absolute shrinkage and selection operator Cox regression analysis, and the coefficients were calculated. The model produced the best data when five FRGs were included ([Figure 3A and B](#)). The coefficient of each FRG is shown in [Figure 3C](#). The prognosis signature was constructed based on five FRGs (*AKR1C1*, *AKR1C3*, *ALOX12*, *CRYAB*, and *FDFT1*). We investigated the genetic alterations of these five FRGs in COAD using the Gene Set Cancer Analysis Lite (<http://bioinfo.life.hust.edu.cn/web/GSCALite/>). The interesting genes in COAD were altered in 15 of 15 queried samples (100%) ([Figure 3D](#)). The frequent genetic alterations demonstrated the essential roles of these FRGs in the development of COAD. In addition, *AKR1C1* mainly participated in the regulation of epithelial-mesenchymal transition (EMT) and hormone androgen receptor activity. *AKR1C3* is mainly involved in the regulation of RAS/MAPK activity, and *CRYAB* is mainly associated with the regulation of EMT and hormone estrogen receptor activity. *FDFT1* mainly participated in the regulation of hormone androgen receptor activity ([Figure 3E](#)). To further explore the association between the expression of each gene and COAD, we applied the “FUNCTIONS-Expression Analysis-Survival Analysis” module of the webserver GEPIA2 to obtain the significance profile data between these five FRGs and OS in COAD. We used the values of cutoff-high (50%) and cutoff-low (50%) as the expression thresholds to divide the patients into high- and low-expression groups. The log-rank test was utilized in the hypothesis test, and survival curves were also acquired *via* the “Survival Analysis” module of the web database GEPIA2. The results indicated that the expression of *AKR1C1*, *AKR1C3*, and *ALOX12* did not have a significant correlation with the OS of COAD (all $P > 0.05$, [Figure 3F-H](#)). High expression of *CRYAB* was correlated with poor OS in COAD ($P < 0.05$, [Figure 3I](#)), while high expression of *FDFT1* was associated with better OS in COAD ($P < 0.05$, [Figure 3J](#)).

A prognostic model of five FRGs was explored according to the optimal value of λ ([Figure 3A and B](#)). The risk score for each patient was calculated based on the following formula: Risk score = $0.5325 \times$ expression level of *AKR1C1* + $(-0.2695) \times$ expression level of *AKR1C3* + $0.3471 \times$ expression level of *ALOX12* + $0.1274 \times$ expression level of *CRYAB* + $(-0.5013) \times$ expression of *FDFT1*.

The risk score was utilized to predict prognosis. Using the median cut-off value, patients were divided into a high-risk group ($n = 177$) and a low-risk group ($n = 178$) ([Figure 4A](#)). Kaplan-Meier cumulative curves showed that patients in the high-risk group had a significantly poorer OS than those in the low-risk group ($P < 0.001$, [Figure 4B](#)). The patients in the high-risk group were significantly correlated to advanced TNM stage in the TCGA-COAD cohort ([Table 2](#)). The principal component analysis and t-distributed stochastic neighbor embedding analysis demonstrated that the patients in diverse risk groups were distributed in two directions ([Figure 4C and D](#)). The survival time diminished as the risk score increased, and a higher risk score corresponded to more deaths in TCGA-COAD ([Figure 4E](#)). A time-dependent ROC analysis was used to further assess the prognostic accuracy of the prognostic model. The AUC value was 0.661 at 1 year, 0.699 at 2 years, and 0.700 at 3 years, which showed a moderate diagnostic ability ([Figure 4F](#)).

Validation of the prognostic model of five FRGs in the GSE39582 cohort

To verify the stability of the signature determined by the TCGA-COAD cohort, patients from the GSE39582 database were also classified as high or low risk, with the median value computed using the same formula as that from the TCGA-COAD dataset ([Figure 5A](#)). Similar to the results obtained from the TCGA-COAD database, the OS of patients in the high-risk group was significantly worse than that of patients in the low-risk group ($P < 0.01$, [Figure 5B](#)). The high-risk group was also associated with advanced TNM stage in the GEO-GSE39582 cohort ([Table 2](#)). The principal component analysis and t-distributed stochastic neighbor embedding analysis showed that patients in the high-risk and low-risk groups were also distributed in discrete directions ([Figure 5C and D](#)). Similarly, an elevated risk score was correlated with a decreased survival time and an increase in mortality ([Figure 5E](#)). In addition, the AUC

Table 2 Baseline features of the colon adenocarcinoma patients in different risk groups, *n* (%)

Features	TCGA-COAD cohort			GEO-GSE39582 cohort		
	High-risk	Low-risk	<i>P</i> value	High-risk	Low-risk	<i>P</i> value
Age			0.795			0.862
< 65 yr	70 (39.5)	68 (38.2)		105 (37.4)	107 (38.1)	
≥ 65 yr	107 (60.5)	110 (61.8)		176 (62.6)	174 (61.9)	
Sex			0.265			0.351
Female	86 (48.6)	76 (42.7)		132 (47.0)	121 (43.1)	
Male	91 (51.4)	102 (57.3)		149 (53.0)	160 (56.9)	
TNM-stage			<i>P</i> < 0.001			<i>P</i> = 0.002
I and II	83 (46.9)	114 (64.0)		134 (47.7)	170 (60.5)	
III and IV	89 (50.3)	58 (32.6)		145 (51.6)	109 (38.8)	
Unknown	5 (2.8)	6 (3.4)		2 (0.7%)	2 (0.7%)	

TCGA-COAD: The Cancer Genome Atlas database-colon adenocarcinoma; GEO: Gene Expression Omnibus.

value of the five FRG signatures was 0.590 at 1 year, 0.598 at 2 years, and 0.558 at 3 years in the GSE39582 cohort (Figure 5F).

Independent prognostic value of the five-FRG signature

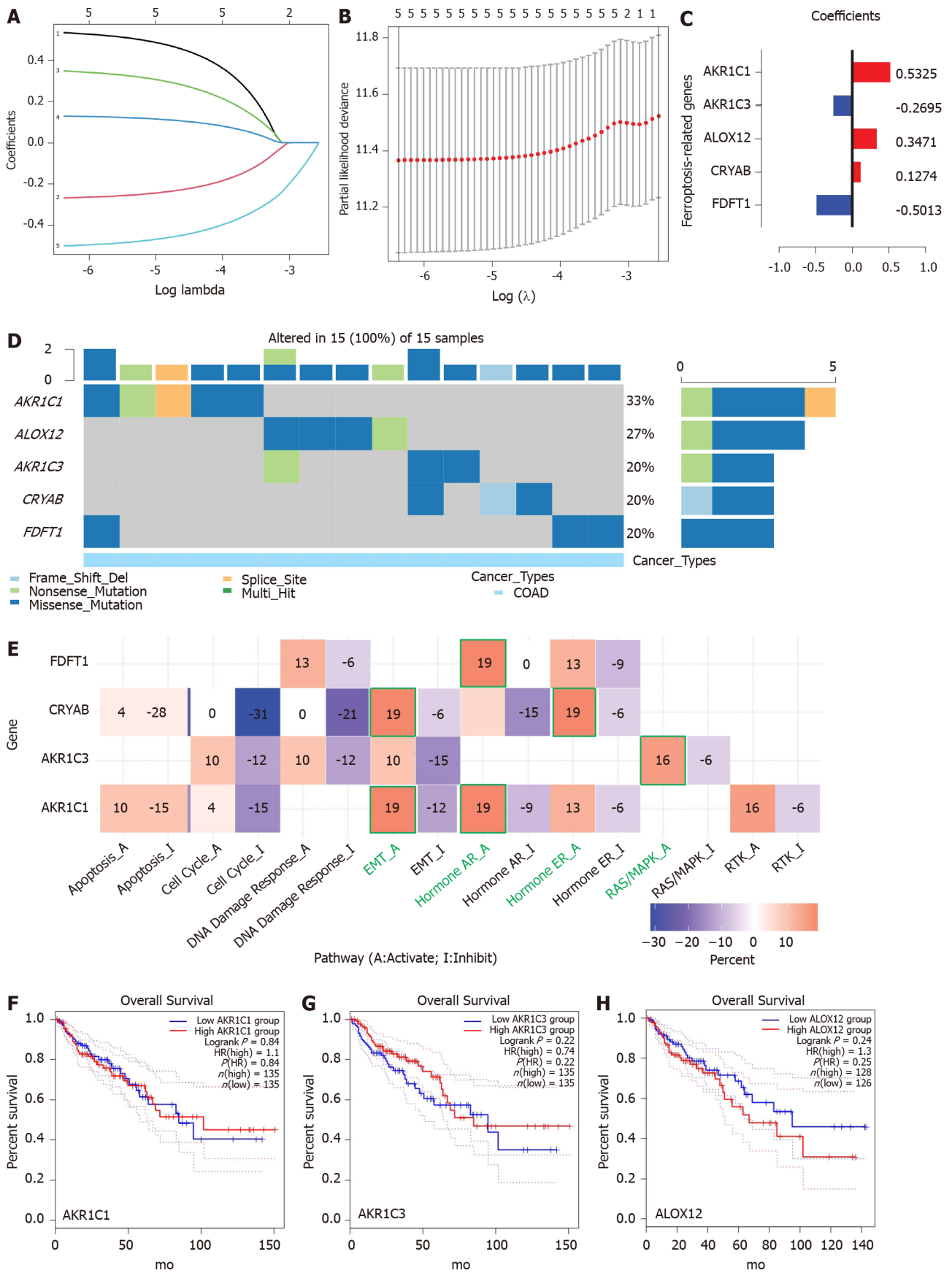
To identify whether the risk score was an independent prognostic factor for OS, we performed univariate and multivariate Cox regression analyses among the available variables. The risk score was remarkably related to OS in both the TCGA and GSE39582 cohorts in the univariate Cox regression analysis (HR = 2.813, *P* < 0.001; HR = 12.008, *P* = 0.002, respectively, Figure 6A-C). After adjustment for other farrago elements, the risk score was confirmed as an independent predictor of OS in the multivariate Cox analysis (TCGA-COAD cohort: HR = 3.934, *P* < 0.001; GSE39582 cohort: HR = 3.632, *P* = 0.002; Figure 6B-D).

Construction of a nomogram based on the five crucial FRGs

A nomogram can quantitatively identify an individual's clinical risk by combining multiple risk factors[33]. We used the nomogram to predict the probability of 1-, 3-, and 5-year OS by merging the five FRG signatures for TCGA-COAD (Figure 7A). The distribution point of each FRG was proportional to its risk contribution to survival and was normalized to the distribution of 0 to 100. We calculated each patient's total points by summarizing the number of points for all FRGs and estimated the survival rates by drawing a vertical line between each prognosis axis and the total point axis. This tool may help practitioners make clinical decisions for COAD patients. The calibration curve demonstrated that the actual survival rate matched the predicted 1-, 3-, and 5-year survival rate (Figure 7B-D). The consistency index was 0.764 in the TCGA-COAD cohort.

Immune correlation analysis between the immune status and risk score

The scores of macrophages, neutrophils, and Th2 cells were considerably different between the high- and low-risk groups in the TCGA-COAD dataset. Macrophages and neutrophils scored higher in the high-risk group, while Th2 cells scored higher in the low-risk group (*P* < 0.05, Figure 8A). The Type II interferon (IFN) Response score was significantly higher in the high-risk group than the low-risk group (adjusted *P* < 0.05, Figure 8B). Comparisons in the GSE39582 cohort showed that the scores of B cells, CD8⁺ T cells, dendritic cells, macrophages, mast cells, neutrophils, plasmacytoid dendritic cells, T helper cells, Thf cells, Th1 cells, and tumor infiltrating lymphocytes were significantly higher in the high-risk group than the low-risk group (adjusted *P* < 0.05, Figure 8C). The scores of antigen presenting cell coinhibition, CC chemokine receptor, checkpoint, cytolytic activity, human leukocyte antigen, inflammation promotion, parainflammation, T cell coinhibition, T cell costimulation, type I IFN response, and type II IFN response were significantly different between the two risk groups (*P* < 0.05, Figure 8D). In particular, the scores of macrophages, neutrophils, and



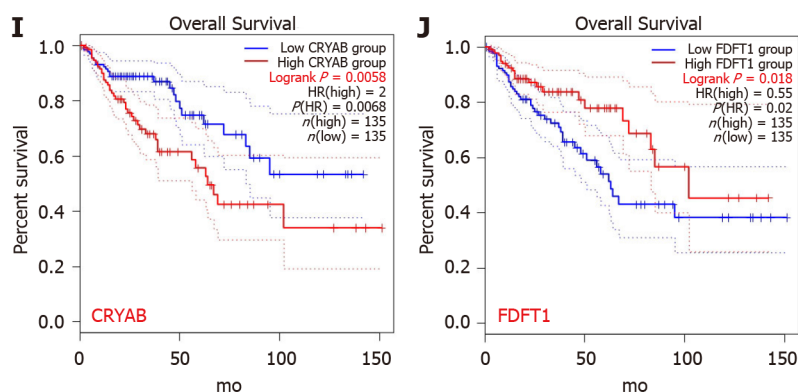


Figure 3 Establishment of a prognostic ferroptosis-related gene signature by least absolute shrinkage and selection operator Cox regression analysis. A-C: Process of constructing the signature including five ferroptosis-related genes. A coefficient profile plot (C) was generated against the log (λ) sequence (A); B: Selection of the optimal parameter (λ) in the least absolute shrinkage and selection operator model for colon adenocarcinoma; D: Genetic alteration of the five genes in colon adenocarcinoma using Gene Set Cancer Analysis. The X axis represents the cancer type, and sky blue indicates colon adenocarcinoma. The left Y axis represents the ratio of gene mutations, and the right Y axis represents the gene names. Different-colored small rectangles indicate the type of gene mutation; E: Four ferroptosis-related genes involved in the regulation of signaling pathways using Gene Set Cancer Analysis. The green pathway names indicate the pathway with the highest proportion of regulation of each gene; F: Single-gene survival analysis of the five ferroptosis-related genes based on the web database GEPIA2. COAD: Colon adenocarcinoma; EMT: Epithelial-mesenchymal transition; AR: Androgen receptor; ER: Estrogen receptor.

type II IFN response were significantly different between the two risk groups in both the TCGA-COAD and GSE39582 cohorts.

Exploring and validation of the expression level of five hub FRGs

The GEPIA2 analysis indicated that the expression levels of *AKR1C1*, *ALOX12*, and *CRYAB* in the tissues of COAD were lower than those in the matching normal tissues (Figure 9A-C). In contrast, the expression levels of *AKR1C3* and *FDFT1* in the tumor tissues of COAD were higher than those in the corresponding normal tissues (Figure 9D-F).

The immunohistochemistry results of the Human Protein Atlas database were used to explore the expression of the five hub FRGs in COAD, and the results showed that *AKR1C1*, *ALOX12*, and *CRYAB* were highly expressed in normal tissues compared with matching tumor tissues (Figure 9G-L). Furthermore, the protein expression of *AKR1C3* was not significantly different between normal and COAD tissues (Figure 9M and N). *FDFT1* was highly expressed in both normal and COAD tissues (Figure 9O and P).

Functional enrichment and KEGG pathway analysis

GO enrichment and KEGG pathway analyses were performed to identify the biological functions and pathways related to the risk score and DEFGRs between the high-risk and low-risk groups. The GO enrichment analysis showed that these genes might be involved in the regulation of several essential biological processes, including muscle contraction, extracellular matrix organization, extracellular structure organization, muscle system process, and regulation of vasculature development. In addition, these genes also participated in the regulation of several molecular functions, such as actin binding, endopeptidase regulator activity, and peptidase regulator activity (Figure 10A). The KEGG pathway analysis indicated that the DEFGRs were mainly involved in the regulation of chemical carcinogenesis and complement and coagulation cascade pathways (Figure 10B).

DISCUSSION

Ferroptosis is a new type of cell death with unique capabilities and identifies functions related to cancers[19]. Recent research shows that ferroptosis has been consistently accepted as a recognized function to eliminate malignant cells, thereby demonstrating its key role in inhibiting tumorigenesis by eliminating cells from the environment that lack key nutrients[34]. More clues about the role of ferroptosis can be obtained from the latest studies of TP53. Xie *et al*[35] found that CRC was resistant to ferroptosis, leading to suppression of dipeptidyl-peptidase-4 activity *via* TP53 as a transcription-

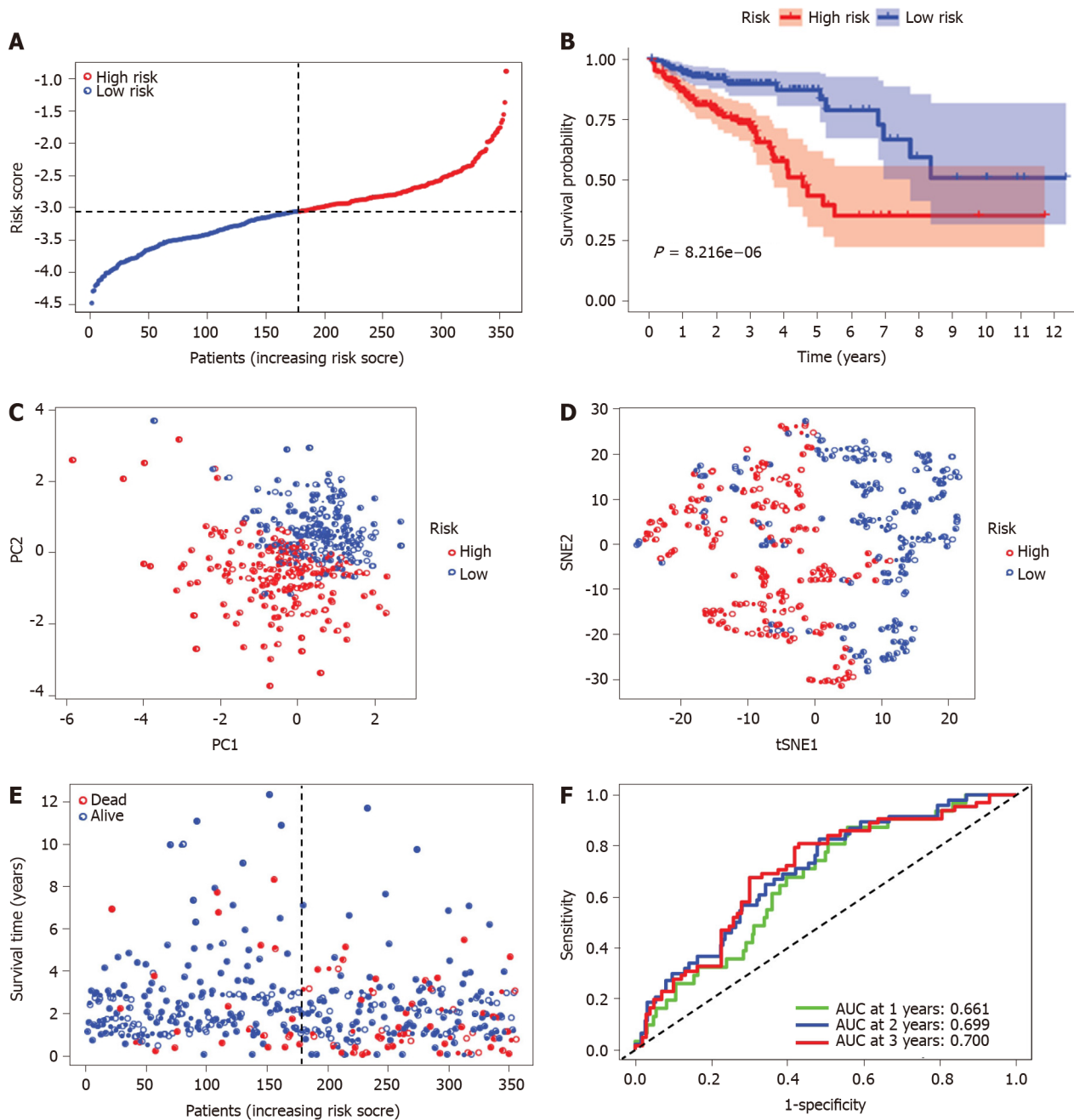


Figure 4 Prognostic analysis of the five ferroptosis-related gene models in the Cancer Genome Atlas-colon adenocarcinoma cohort. A: Distribution and median value of the risk scores in the Cancer Genome Atlas-colon adenocarcinoma (TCGA-COAD) cohort. The black dotted line is the optimum cut-off dividing patients into high-risk and low-risk groups. The red curve represents high risk, and the blue curve represents low risk; B: Kaplan-Meier survival curves for the overall survival of patients in the high-risk group and low-risk group in the TCGA-COAD cohort; C: Principal component analysis plot of the TCGA-COAD cohort; D: t-distributed stochastic neighbor embedding analysis of the TCGA-COAD cohort; E: Distributions of overall survival status, overall survival, and risk score in the TCGA-COAD cohort. The red dot indicates patient death, and the blue dot indicates patient survival; F: Area under the curve values of time-dependent receiver operating characteristic curves verified the prognostic performance of the risk score in the TCGA-COAD cohort. PC: Principal component analysis; t-SNE: t-distributed stochastic neighbor embedding; AUC: Area under the curve.

independent method. *TP53* loss increases the dipeptidyl-peptidase-4 concentration at the plasma membrane and thus enhances dipeptidyl-peptidase-4-dependent lipid peroxidation, ultimately leading to ferroptotic cell death. In the current research, we comprehensively investigated the expression of 60 FRGs in COAD tumor tissues and their relationship to OS. A new prognostic signature based on five FRGs was constructed and validated in an outside dataset.

Although a few previous studies[36-38] have demonstrated that certain genes may be associated with drug-induced ferroptosis in COAD, the association with the OS of COAD patients is still largely unknown. Impressively, most of the FRGs (85%) were differentially expressed between corresponding adjacent non-neoplastic tissues and

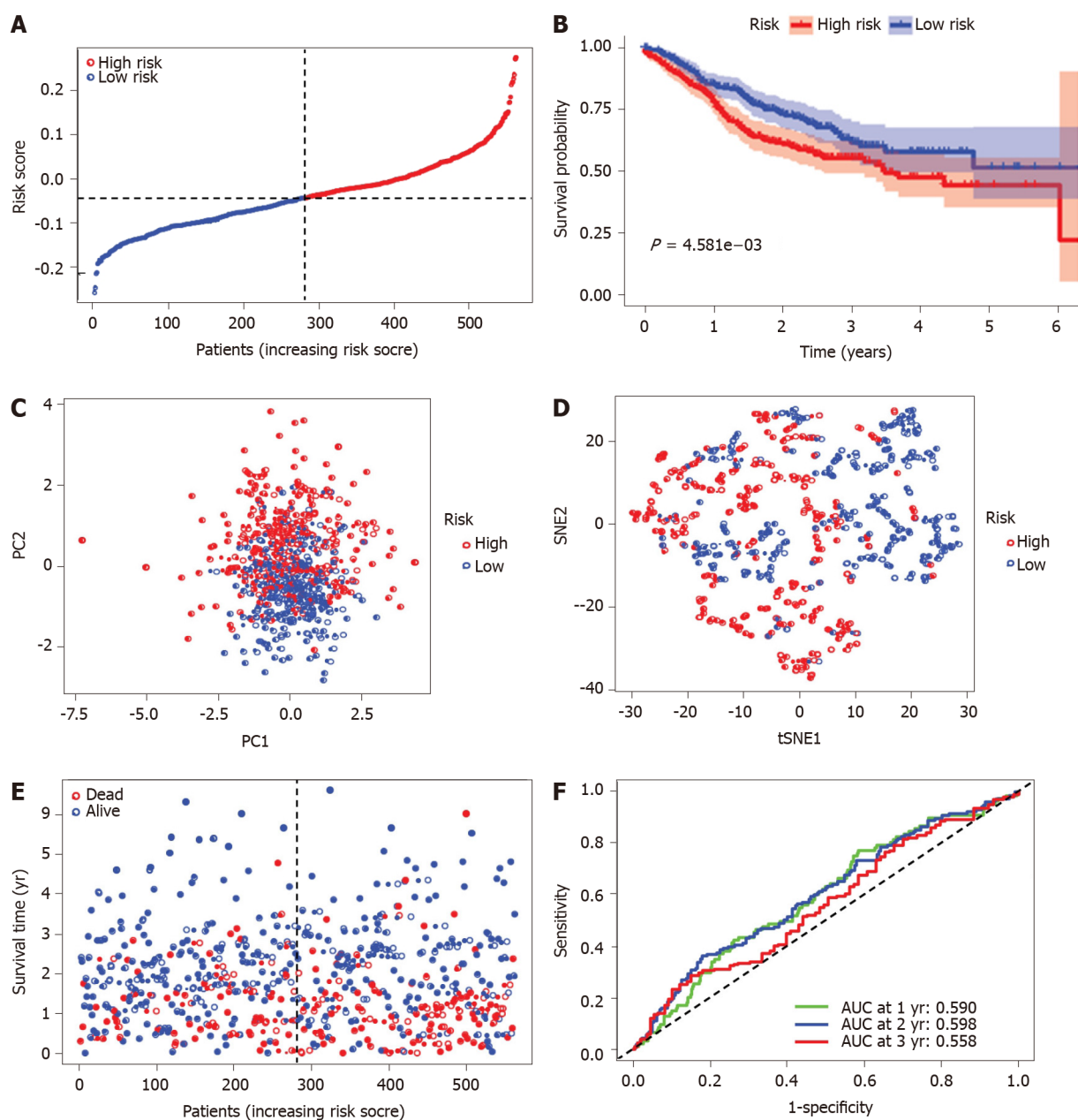


Figure 5 Prognostic analysis of the five ferroptosis-related gene models in the GSE39582 cohort. A: Distribution and median value of the risk scores in the GSE39582 cohort. The black dotted line is the optimum cut-off dividing patients into high-risk and low-risk groups. The red curve represents high risk, and the blue curve represents low risk; B: Kaplan-Meier survival curves for the overall survival of patients in the high-risk group and low-risk group in the GSE39582 cohort; C: Principal component analysis plot of the GSE39582 cohort; D: t-distributed stochastic neighbor embedding analysis of the GSE39582 cohort; E: Distribution of overall survival status, overall survival, and risk score in the GSE39582 cohort. The red dot indicates patient death, and the blue dot indicates survival; F: Area under the curve values of time-dependent receiver operating characteristic curves verified the prognostic performance of the risk score in the GSE39582 cohort. PCA: Principal component analysis; t-SNE: t-distributed stochastic neighbor embedding; AUC: Area under the curve.

COAD tissues. These results demonstrated the underlying role of ferroptosis in COAD and the possibility of constructing a prognostic signature based on these FRGs.

First, we attempted to construct a prognostic model for COAD patients based on five FRGs (*AKR1C1*, *AKR1C3*, *ALOX12*, *CRYAB*, and *FDFT1*) screened by a least absolute shrinkage and selection operator Cox regression analysis and identified the risk score. The prognostic signature is precise and has an accurate predictive advantage. We found that the risk score was an independent prognostic element. *AKR1C1* (aldo-keto reductase family 1 member C1) encodes a member of the aldo/keto reductase superfamily. Concurrent *STK11/KEAP1* mutations led to considerable upregulation of ferroptosis-protective genes (*AKR1C1/2/3*) and resistance to pharmacologically induced ferroptosis in lung cancer. In the pathway analysis, we found that *AKR1C1* mainly participated in the regulation of EMT. Previous research has shown that aldo-keto reductases protect metastatic melanoma from estrogen

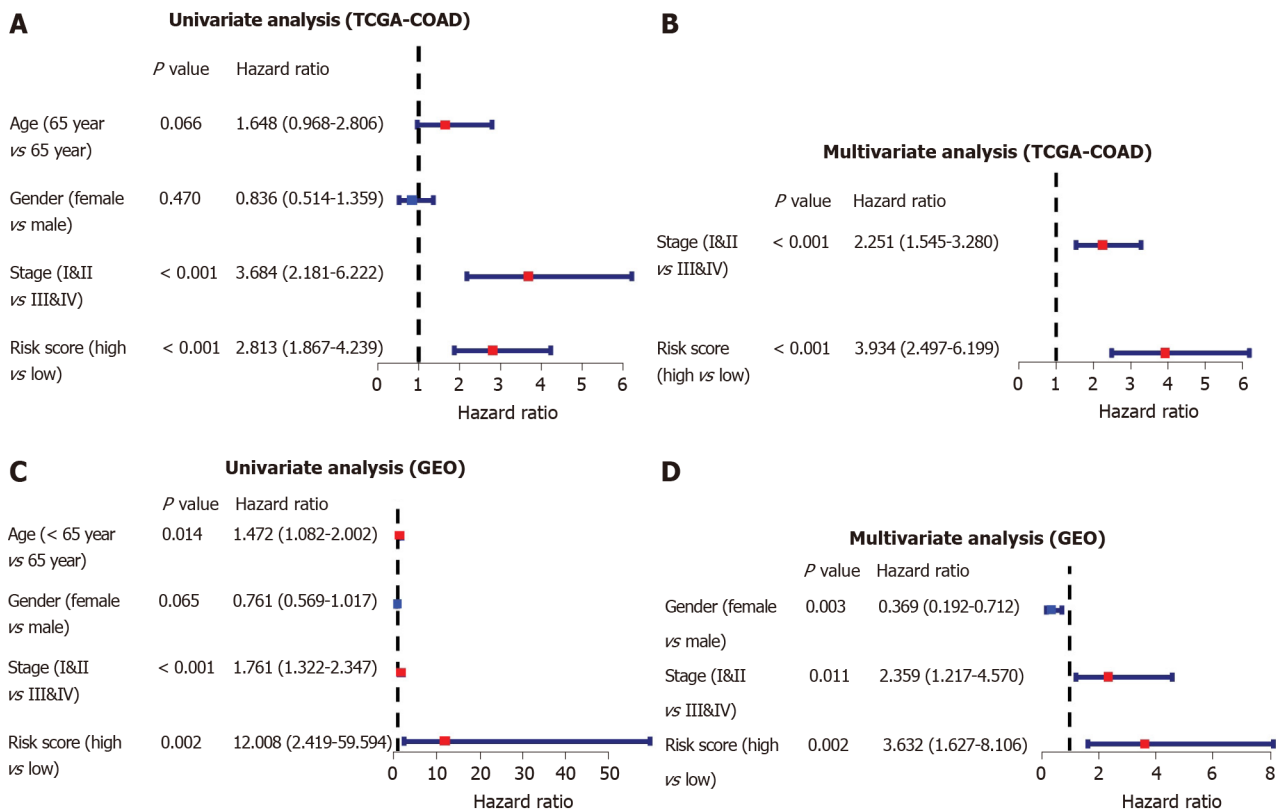


Figure 6 Independent prognostic value analysis of the five ferroptosis-related gene signatures. A: Univariate Cox regression analyses in the Cancer Genome Atlas training cohort; B: Multivariate Cox regression analyses in the Cancer Genome Atlas training cohort; C: Gene Expression Omnibus validation cohort; D: Gene Expression Omnibus validation cohort. TCGA-COAD: The Cancer Genome Atlas database-colon adenocarcinoma; GEO: Gene Expression Omnibus.

receptor stress-independent ferroptosis due to the EMT-related gene expression reprogramming process[39].

ALOX12, an arachidonate 12-lipoxygenase-encoding enzyme, acts on diverse polyunsaturated fatty acid substrates to produce bioactive lipid mediators containing lipoxins and eicosanoids. Loss of one *ALOX12* allele is sufficient to expedite tumorigenesis in E μ -Myc lymphoma models. *ALOX12* is not necessary for ferroptosis induced by GPX4 or erastin inhibitors, whereas *ACSL4* is necessary for ferroptosis upon GPX4 inhibition but not necessary for TP53-mediated ferroptosis[40]. Inhibition of *ALOX12* in SW620 cells or blood endothelial cells attenuated circular chemorepellent-induced defects[41]. In addition, genetic variation in *ALOX12* could influence the risk of rectal cancer and an association may occur between nonsteroidal anti-inflammatory drug use and variants in *ALOX12* on CRC risk[42].

CRYAB is a member of the small heat shock protein family and interacts with TP53 to isolate its translocation to mitochondria, thereby indirectly constraining its proapoptotic influence on apoptotic Bcl-2 molecules[43]. Previous reports indicated that CRC patients with high expression of *CRYAB* and positive distant metastasis showed significantly reduced OS. High *CRYAB* expression could promote tumor cell proliferation, invasion, and metastasis of CRC by EMT[44,45]. These results are consistent with our study, in which *CRYAB*, as a high-risk gene, is mainly associated with the regulation of EMT activity and higher expression of *CRYAB* is related to poor OS in COAD.

FDFT1 encodes a membrane-associated enzyme located at a branch point in the mevalonate pathway. Weng *et al*[46] reported that the downregulation of *FDFT1* is related to malignant progression and poor prognosis in CRC and that *FDFT1* acts as an essential cancer suppressor in CRC, which is consistent with our result showing that high *FDFT1* expression is associated with better OS in COAD.

In summary, three of the genes (*AKR1C1*, *AKR1C3*, and *ALOX12*) in the prognostic signature have been clarified to protect cells from ferroptosis, whereas the relationship between the two surplus genes (*CRYAB* and *FDFT1*) and ferroptosis has not been reported. Whether these genes play a role in the prognosis of COAD patients by affecting the course of ferroptosis remains to be clarified because few associated

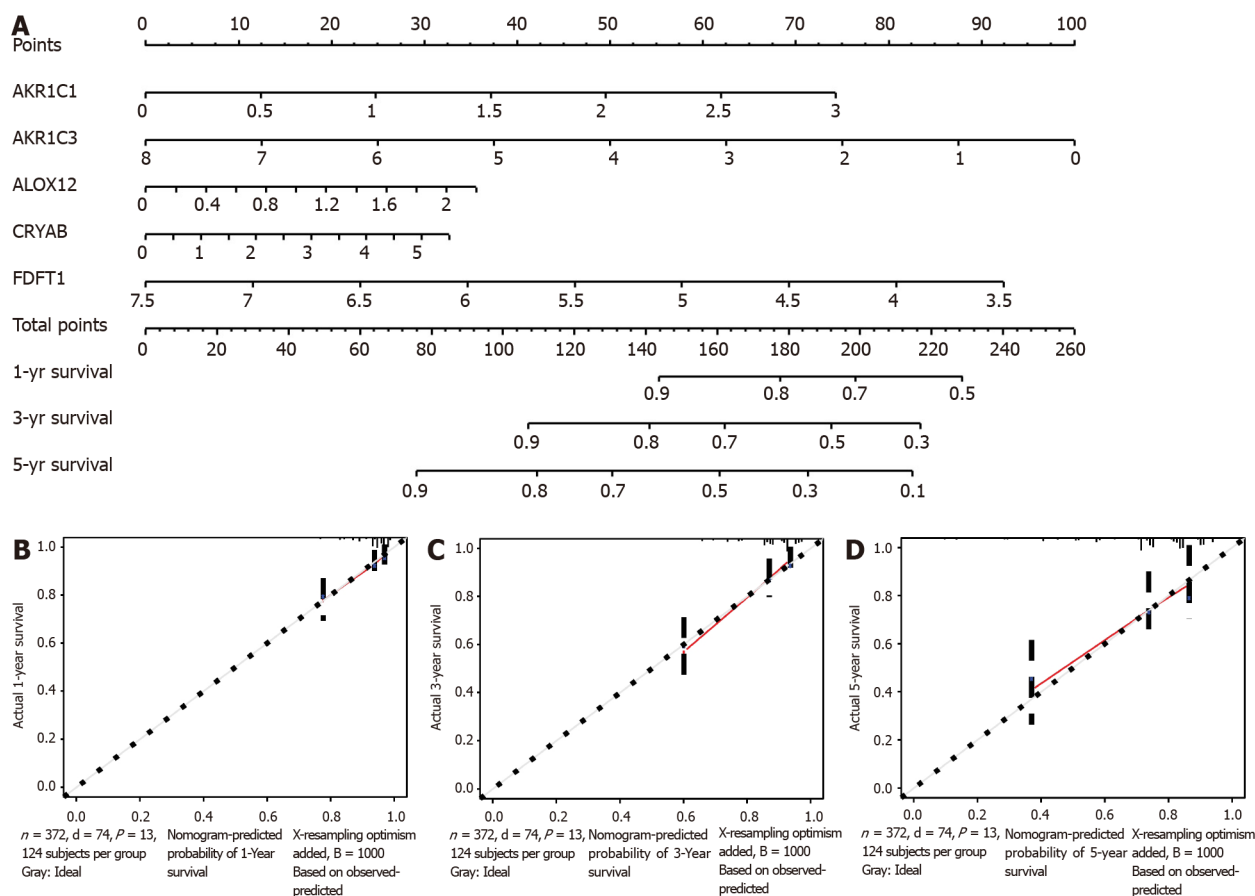


Figure 7 Nomogram for predicting the prognostic ability of The Cancer Genome Atlas database-colon adenocarcinoma. A: Nomogram for predicting 1-, 3-, and 5-year overall survival of colon adenocarcinoma by the expression of the five ferroptosis-related genes; B-D: 1-, 3-, and 5-year calibration curves of the Cancer Genome Atlas database-colon adenocarcinoma. The X axis represents the predicted survival time, and the Y axis demonstrates the actual survival time.

studies on these genes (except for *AKR1C1* and *AKR1C3*) have been reported.

Whether the expression level of FRGs can be applied as a prognostic marker is an essential subject for study. Our COAD prognostic signature based on five FRGs was discovered to be valuable, and the scores of 1-, 3-, and 5-year risk and the AUC value of the ROC curve were consistent with previous studies[47-50]. The prognoses were divided into high-risk and low-risk groups, and the five FRGs we selected may be ideal prognostic markers. In the high-risk group, the 5-year OS was approximately 43% and 85% in the low-risk group, which is consistent with previous research[51]. In addition, we constructed a nomogram to predict the clinical prognosis of individual COAD patients. A nomogram is a reliable and steady tool to quantify the risk of individual patients by integrating and describing risk elements, and this tool has been applied for tumor prognosis, including CRC[52,53]. Nomograms produce a graphical statistical forecasting model that can assign scores to every element. Risk scores based on genetic markers can be included in a predictive nomogram model to predict clinical prognosis. A combination of metabolism-related gene markers and a prognostic element has better prognostic value than an individual marker for CRC[52]. We were able to show that a nomogram, including the five FRGs signature, could better predict 1-, 3-, and 5-year survival possibility of COAD patients. These results showed that the five FRG prognostic model is of value in determining the treatment plan of COAD patients.

In recent years, the mechanisms underlying tumor susceptibility to ferroptosis have been a hot area of study; however, the potential regulatory role between tumor immunity and ferroptosis has not been clarified. Macrophages and neutrophils scored higher in the high-risk group, while Th2 cells scored higher in the low-risk group. Previous studies have indicated that tumor-associated macrophages correlate with shorter survival in colon cancer[54] because of their role in immune invasion. Neutrophils also promote the spread of tumor cells by using neutrophilic extracellular traps to capture circulating CRC cells and promote their distant migration[55].

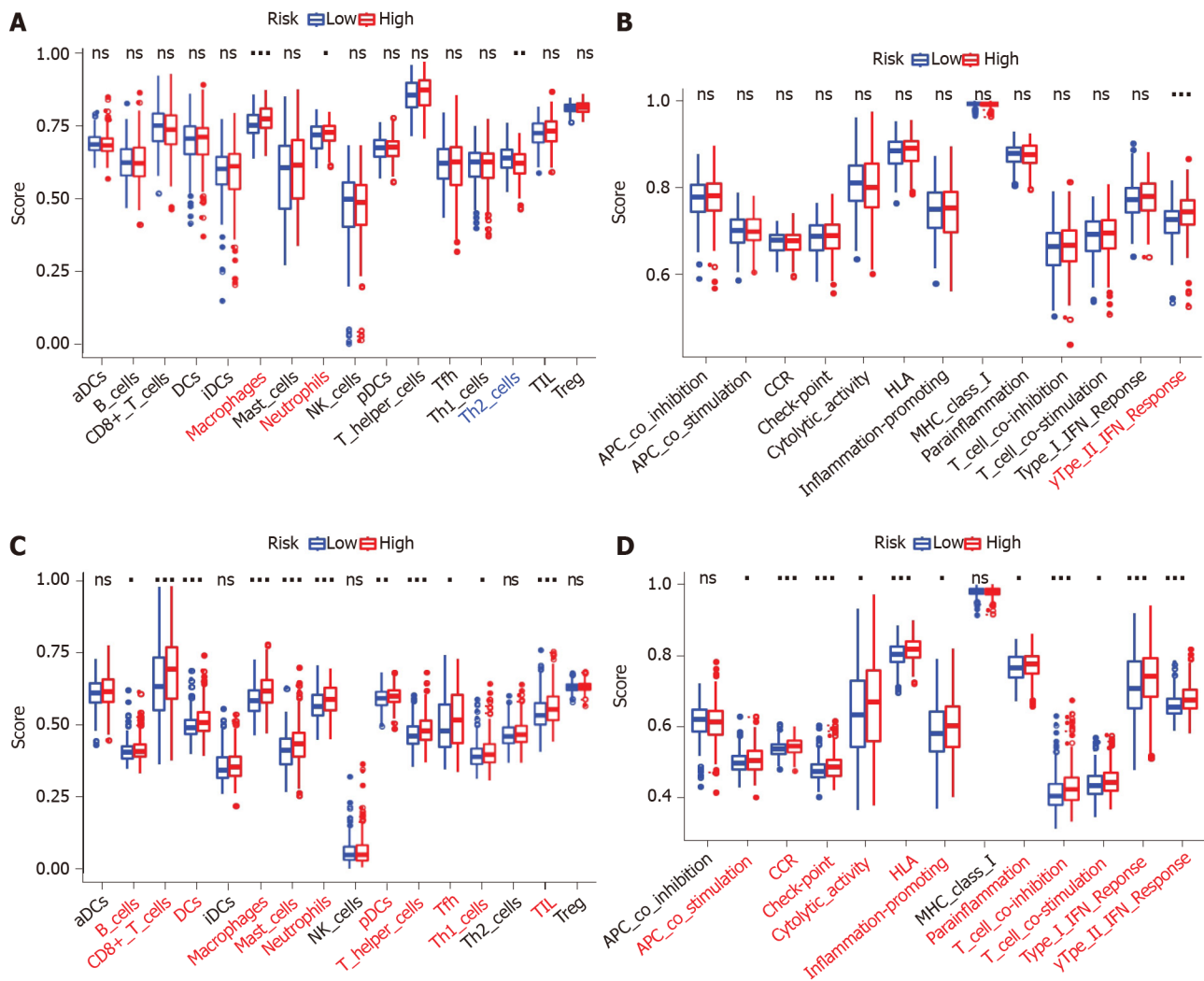
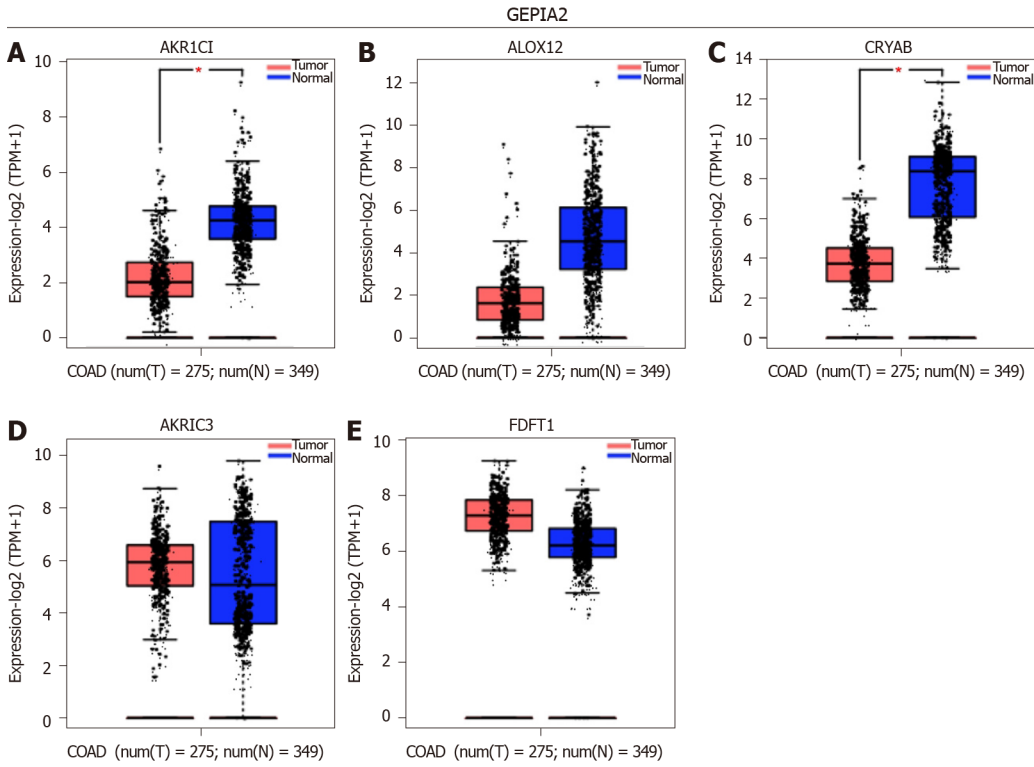


Figure 8 Comparison of the single sample gene set enrichment analysis scores between different risk groups in the Cancer Genome Atlas-colon adenocarcinoma database cohort and GSE39582 cohort. A and C: Scores of 16 immune cells; B and D: 13 immune-related functions are shown in boxplots. Adjusted *P* values are indicated as follows: ^a*P* < 0.05; ^b*P* < 0.01; ^c*P* < 0.001. ns: Not significant. aDC: Activated dendritic cell; DC: Dendritic cell; iDC: Immature dendritic cell; NK: Natural killer; pDC: Plasmacytoid dendritic cell; TIL: Tumor infiltrating lymphocyte; Treg: Regulatory T cell; APC: Antigen presenting cell; CCR: CC chemokine receptor; HLA: Human leukocyte antigen; MHC: Major histocompatibility complex; IFN: Interferon.

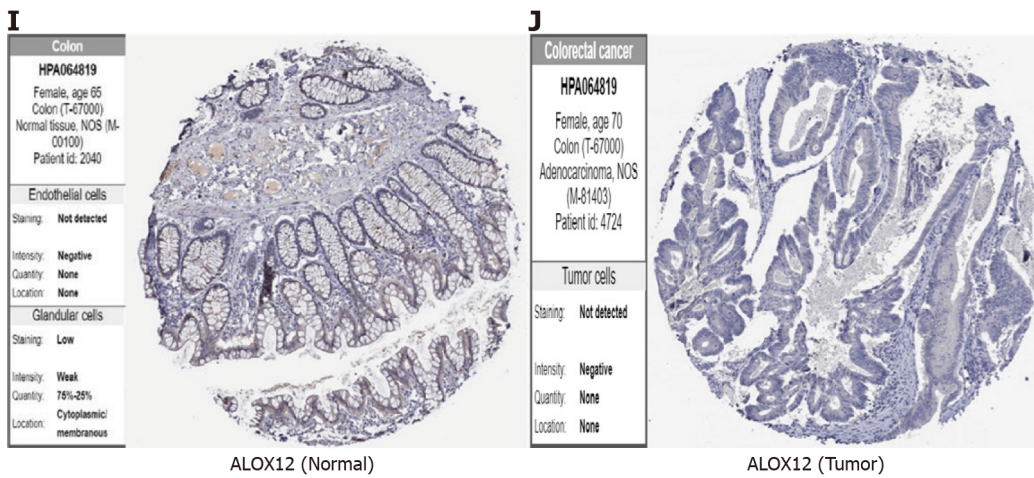
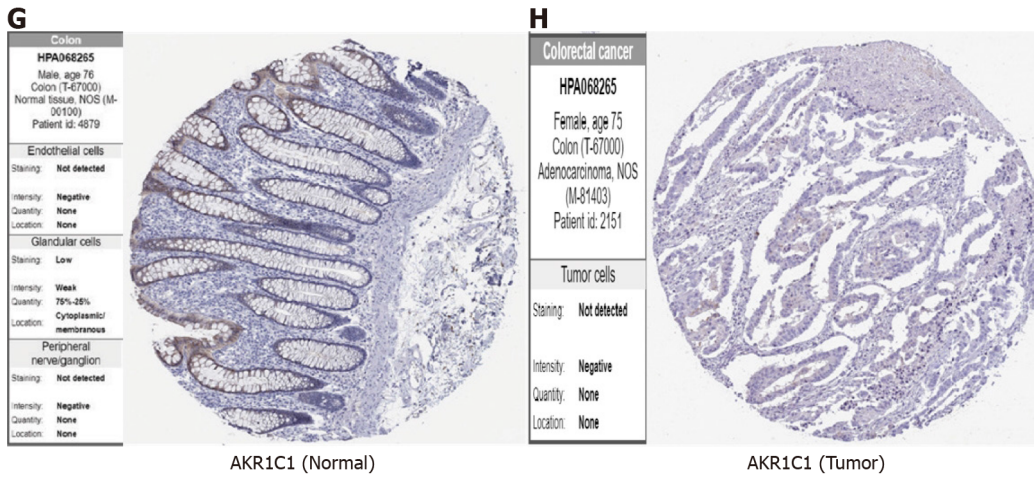
Epithelial notch signaling recruits neutrophils to drive colon cancer metastasis[56]. In addition, higher risk scores related to impaired antitumor immunity included the activity of the type II IFN response. In addition, the type II IFN response is involved in the recurrence of lower grade glioma[57]. Therefore, weakened antitumor immunity in high-risk patients may be one of the reasons for their poor prognosis.

Based on the differentially expressed FRGs between the high- and low-risk groups, we performed a GO analysis and surprisingly found that several EMT-associated biological processes and pathways were enriched. Therefore, a rational assumption is that ferroptosis is closely related to EMT. Interestingly, there was a significant difference in the content of the antigen presentation process between the high-risk and low-risk groups in this research.

Although a prognostic model based on the five FRGs was constructed and the risk score was an independent prognostic marker for OS in COAD, our research still has some shortcomings. First, this research mainly focused on performing a bioinformatic analysis of retrospective data from public databases. In the future, more prospective real-world data are needed to confirm the clinical utility of the findings. Second, although FRG expression was discovered to be associated with the tumor immune cell infiltration level and patient survival, we were unable to identify whether FRGs affect patient survival through immune cell infiltration. Future prospective studies should focus on the expression of these FRGs and infiltration of immune cells in COAD, which may help provide more mechanistic insights associated with this problem.



HPA



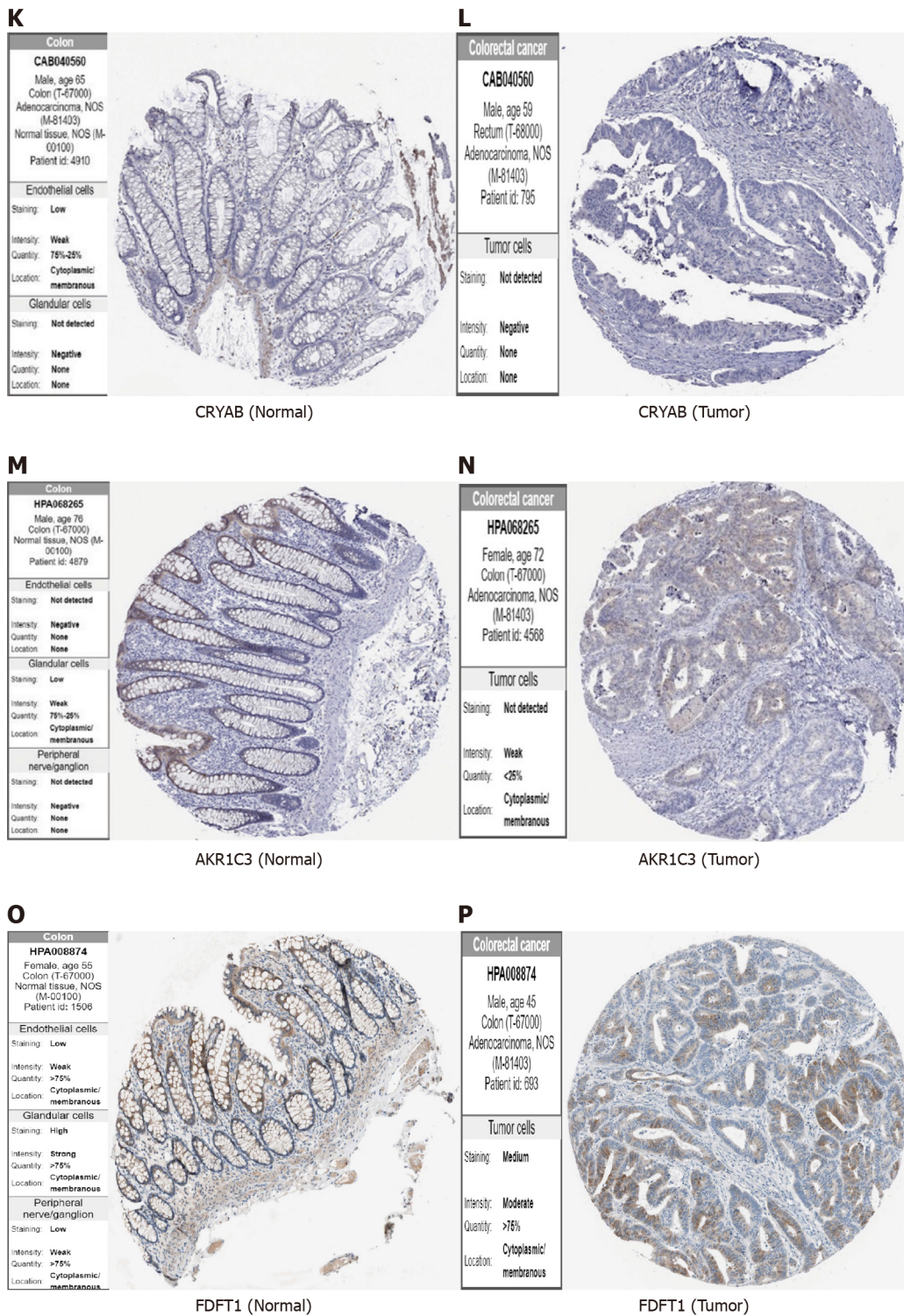


Figure 9 Validation of the expression of five core ferroptosis-related genes and corresponding proteins in colon adenocarcinoma tissues and corresponding adjacent normal tissues. The gene expression levels of *AKR1C1* (A), *ALOX12* (B), *CRYAB* (C), *AKR1C3* (D), and *FDFT1* (E) in colon adenocarcinoma and the corresponding normal tissues of Genotype-tissue expression and the Cancer Genome Atlas database by GEPIA2 (F). The protein expression levels of *AKR1C1* (G and H), *ALOX12* (I and J), *CRYAB* (K and L), *AKR1C3* (M and N), and *FDFT1* (O and P) in colon adenocarcinoma and the corresponding normal tissues by the Human Protein Atlas database. COAD: Colon adenocarcinoma; HPA: Human Protein Atlas.

CONCLUSION

In summary, our research defined a new prognostic signature with five FRGs in COAD. The FRG signature proved to be independently related to OS in both the training and validation datasets, thus providing insights into prognostic predictions for COAD. The potential mechanisms between FRGs and tumor immunity in COAD are still poorly understood and need to be further investigated. These results provided

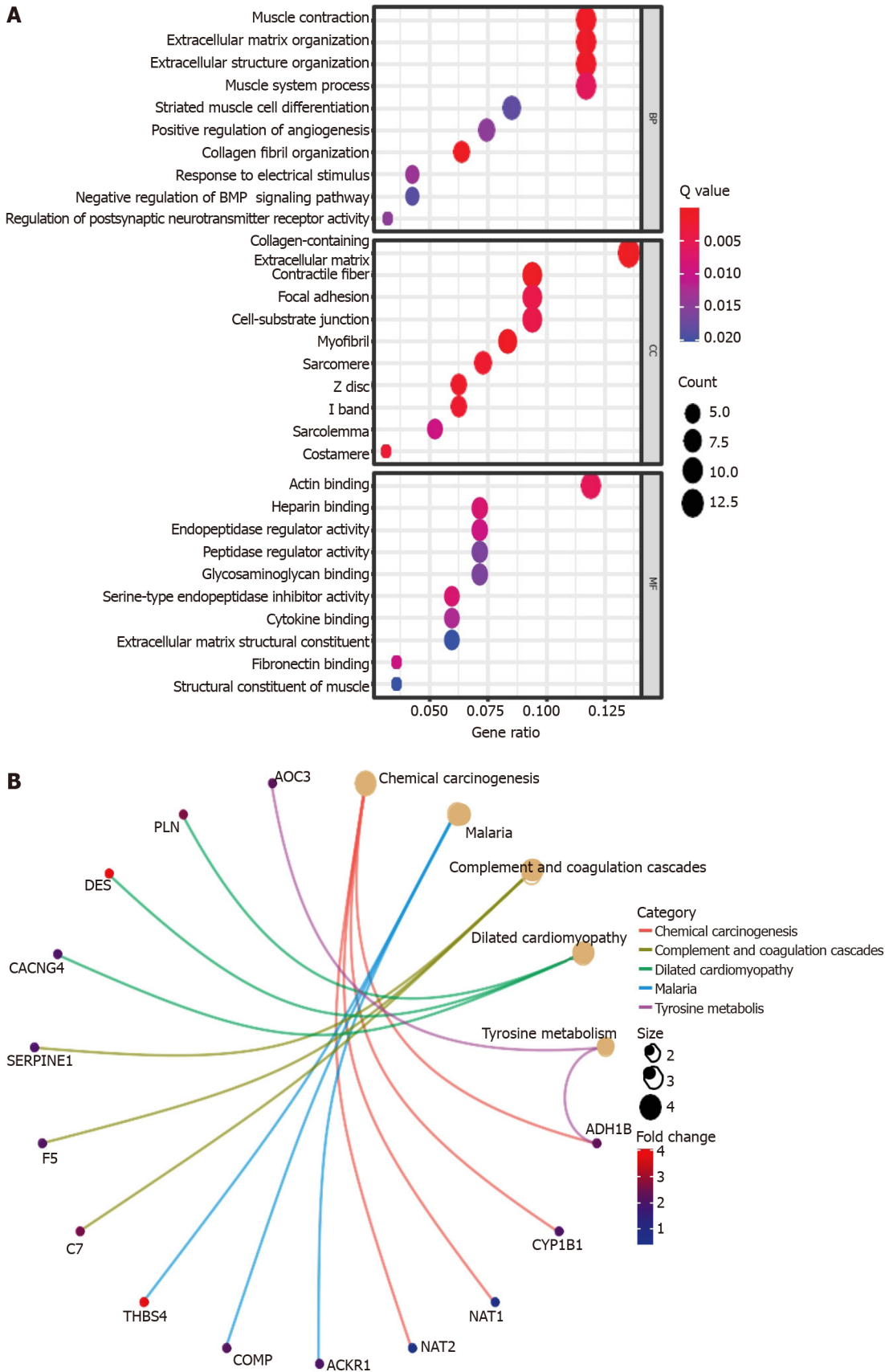


Figure 10 Representative results of the Gene Ontology and Kyoto Encyclopedia of Genes and Genomes analyses. The most significant Gene Ontology enrichment (A) and Kyoto Encyclopedia of Genes and Genomes pathways (B) in the Cancer Genome Atlas-colon adenocarcinoma cohort.

a comprehensive perspective for further studies on the role of hub FRGs in the pathogenesis of COAD and identified underlying molecular markers for the diagnosis and treatment of COAD.

ARTICLE HIGHLIGHTS

Research background

Colon adenocarcinoma (COAD) is one of the most common and fatal malignant tumors, which increases the difficulty of prognostic predictions. Ferroptosis is a recently identified programmed cell death process that has the characteristics of iron-dependent lipid peroxide accumulation. However, the predictive value of ferroptosis-related genes (FRGs) for COAD still needs to be further clarified. Therefore, the screening of novel therapeutic targets or prognostic biomarkers based on FRGs could be an essential work for COAD therapy, which could contribute to the improvement of treatment schemes.

Research motivation

This article aims to identify critical FRGs and construct a COAD patient prognostic signature for clinical utilization.

Research objectives

This research addressed the question of the novel FRG gene biomarkers and potential mechanism involved in the development of COAD.

Research methods

The Cancer Genome Atlas database (TCGA) and Gene Expression Omnibus databases were the data sources for mRNA expression and corresponding COAD patient clinical information. Differentially expressed FRGs were recognized using R and Perl software. We constructed a multi-FRG signature of the TCGA-COAD cohort by performing a univariate Cox regression and least absolute shrinkage and selection operator Cox regression analysis. COAD patients from the Gene Expression Omnibus cohort were utilized for verification.

Research results

Most of the FRGs (85%) were differentially expressed between the corresponding adjacent normal tissues and cancer tissues in the TCGA-COAD cohort. Seven FRGs were related to overall survival (OS) in the univariate Cox analysis (all $P < 0.05$). A model with five FRGs (*AKR1C1*, *AKR1C3*, *ALOX12*, *CRYAB*, and *FDFT1*) was constructed to divide patients into high- and low-risk groups. The OS of patients in the high-risk group was significantly lower than that of the low-risk group (all $P < 0.01$ in the TCGA and Gene Expression Omnibus cohorts). The risk score was an independent prognosticator of OS in the multivariate Cox analysis (hazard ratio > 1 , $P < 0.01$). The predictive capacity of the model was verified by a receiver operating characteristic curve analysis. In addition, a nomogram based on the expression of five hub FRGs and risk score can precisely predict the OS of individual COAD cancer patients. Immune correlation analysis and functional enrichment analysis results revealed that immunology-related pathways were abundant, and the immune states of the high-risk group and the low-risk group were different.

Research conclusions

Our research constructed a new prognostic signature with five FRGs in COAD. The FRG signature proved to be independently related to OS in both the training and validation datasets, thus providing insights into prognostic predictions for COAD. Targeting ferroptosis may be a treatment option for COAD.

Research perspectives

In this study, we identified five FRGs signatures in COAD, and this signature proved to be independently related to OS, suggesting that the five FRG signatures might be novel therapeutic targets for COAD. In our subsequent work, the potential mechanisms between FRGs and tumor immunity in COAD will be investigated, which might contribute to the improvement of treatment schemes.

ACKNOWLEDGEMENTS

We acknowledge the Cancer Genome Atlas and Gene Expression Omnibus database for providing their platforms and contributors for uploading their meaningful

datasets. The authors would like to express their gratitude to AJE (www.aje.com) for the expert linguistic services provided. In addition, Yan-Dong Miao would like to give special thanks to Wu-Xia Quan for her patience, care, and support over the past years.

REFERENCES

- 1 **Sung H**, Ferlay J, Siegel RL, Laversanne M, Soerjomataram I, Jemal A, Bray F. Global Cancer Statistics 2020: GLOBOCAN Estimates of Incidence and Mortality Worldwide for 36 Cancers in 185 Countries. *CA Cancer J Clin* 2021; **71**: 209-249 [PMID: 33538338 DOI: 10.3322/caac.21660]
- 2 **Murphy N**, Jenab M, Gunter MJ. Adiposity and gastrointestinal cancers: epidemiology, mechanisms and future directions. *Nat Rev Gastroenterol Hepatol* 2018; **15**: 659-670 [PMID: 29970888 DOI: 10.1038/s41575-018-0038-1]
- 3 **Aune D**, Chan DS, Lau R, Vieira R, Greenwood DC, Kampman E, Norat T. Dietary fibre, whole grains, and risk of colorectal cancer: systematic review and dose-response meta-analysis of prospective studies. *BMJ* 2011; **343**: d6617 [PMID: 22074852 DOI: 10.1136/bmj.d6617]
- 4 **Magalhães B**, Peleteiro B, Lunet N. Dietary patterns and colorectal cancer: systematic review and meta-analysis. *Eur J Cancer Prev* 2012; **21**: 15-23 [PMID: 21946864 DOI: 10.1097/CEJ.0b013e3283472241]
- 5 **O'Keefe SJ**. Diet, microorganisms and their metabolites, and colon cancer. *Nat Rev Gastroenterol Hepatol* 2016; **13**: 691-706 [PMID: 27848961 DOI: 10.1038/nrgastro.2016.165]
- 6 **Sharma R**. An examination of colorectal cancer burden by socioeconomic status: evidence from GLOBOCAN 2018. *EPMA J* 2020; **11**: 95-117 [PMID: 32140188 DOI: 10.1007/s13167-019-00185-y]
- 7 **Lafitte M**, Sirvent A, Roche S. Collagen Kinase Receptors as Potential Therapeutic Targets in Metastatic Colon Cancer. *Front Oncol* 2020; **10**: 125 [PMID: 32117772 DOI: 10.3389/fonc.2020.00125]
- 8 **Meyerson M**, Gabriel S, Getz G. Advances in understanding cancer genomes through second-generation sequencing. *Nat Rev Genet* 2010; **11**: 685-696 [PMID: 20847746 DOI: 10.1038/nrg2841]
- 9 **Liu J**, Lichtenberg T, Hoadley KA, Poisson LM, Lazar AJ, Cherniack AD, Kovatich AJ, Benz CC, Levine DA, Lee AV, Omberg L, Wolf DM, Shriver CD, Thorsson V; Cancer Genome Atlas Research Network, Hu H. An Integrated TCGA Pan-Cancer Clinical Data Resource to Drive High-Quality Survival Outcome Analytics. *Cell* 2018; **173**: 400-416.e11 [PMID: 29625055 DOI: 10.1016/j.cell.2018.02.052]
- 10 **Dixon SJ**. Ferroptosis: bug or feature? *Immunol Rev* 2017; **277**: 150-157 [PMID: 28462529 DOI: 10.1111/immr.12533]
- 11 **Dixon SJ**, Lemberg KM, Lamprecht MR, Skouta R, Zaitsev EM, Gleason CE, Patel DN, Bauer AJ, Cantley AM, Yang WS, Morrison B 3rd, Stockwell BR. Ferroptosis: an iron-dependent form of nonapoptotic cell death. *Cell* 2012; **149**: 1060-1072 [PMID: 22632970 DOI: 10.1016/j.cell.2012.03.042]
- 12 **Stockwell BR**, Friedmann Angeli JP, Bayir H, Bush AI, Conrad M, Dixon SJ, Fulda S, Gascón S, Hatzios SK, Kagan VE, Noel K, Jiang X, Linkermann A, Murphy ME, Overholtzer M, Oyagi A, Pagnussat GC, Park J, Ran Q, Rosenfeld CS, Salnikow K, Tang D, Torti FM, Torti SV, Toyokuni S, Woerpel KA, Zhang DD. Ferroptosis: A Regulated Cell Death Nexus Linking Metabolism, Redox Biology, and Disease. *Cell* 2017; **171**: 273-285 [PMID: 28985560 DOI: 10.1016/j.cell.2017.09.021]
- 13 **Yagoda N**, von Rechenberg M, Zaganjor E, Bauer AJ, Yang WS, Fridman DJ, Wolpaw AJ, Smukste I, Peltier JM, Boniface JJ, Smith R, Lessnick SL, Sahasrabudhe S, Stockwell BR. RAS-RAF-MEK-dependent oxidative cell death involving voltage-dependent anion channels. *Nature* 2007; **447**: 864-868 [PMID: 17568748 DOI: 10.1038/nature05859]
- 14 **Cao JY**, Dixon SJ. Mechanisms of ferroptosis. *Cell Mol Life Sci* 2016; **73**: 2195-2209 [PMID: 27048822 DOI: 10.1007/s00018-016-2194-1]
- 15 **Xie Y**, Hou W, Song X, Yu Y, Huang J, Sun X, Kang R, Tang D. Ferroptosis: process and function. *Cell Death Differ* 2016; **23**: 369-379 [PMID: 26794443 DOI: 10.1038/cdd.2015.158]
- 16 **Xu T**, Ding W, Ji X, Ao X, Liu Y, Yu W, Wang J. Molecular mechanisms of ferroptosis and its role in cancer therapy. *J Cell Mol Med* 2019; **23**: 4900-4912 [PMID: 31232522 DOI: 10.1111/jcmm.14511]
- 17 **Schott C**, Graab U, Cuvelier N, Hahn H, Fulda S. Oncogenic RAS Mutants Confer Resistance of RMS13 Rhabdomyosarcoma Cells to Oxidative Stress-Induced Ferroptotic Cell Death. *Front Oncol* 2015; **5**: 131 [PMID: 26157704 DOI: 10.3389/fonc.2015.00131]
- 18 **Shaw AT**, Winslow MM, Magendanz M, Ouyang C, Dowdle J, Subramanian A, Lewis TA, Maglathin RL, Tolliday N, Jacks T. Selective killing of K-ras mutant cancer cells by small molecule inducers of oxidative stress. *Proc Natl Acad Sci U S A* 2011; **108**: 8773-8778 [PMID: 21555567 DOI: 10.1073/pnas.1105941108]
- 19 **Mou Y**, Wang J, Wu J, He D, Zhang C, Duan C, Li B. Ferroptosis, a new form of cell death: opportunities and challenges in cancer. *J Hematol Oncol* 2019; **12**: 34 [PMID: 30925886 DOI: 10.1186/s13045-019-0720-y]
- 20 **Hassannia B**, Vandenabeele P, Vanden Berghe T. Targeting Ferroptosis to Iron Out Cancer. *Cancer Cell* 2019; **35**: 830-849 [PMID: 31105042 DOI: 10.1016/j.ccell.2019.04.002]

- 21 **Liang C**, Zhang X, Yang M, Dong X. Recent Progress in Ferroptosis Inducers for Cancer Therapy. *Adv Mater* 2019; **31**: e1904197 [PMID: 31595562 DOI: 10.1002/adma.201904197]
- 22 **Jiang L**, Kon N, Li T, Wang SJ, Su T, Hibshoosh H, Baer R, Gu W. Ferroptosis as a p53-mediated activity during tumour suppression. *Nature* 2015; **520**: 57-62 [PMID: 25799988 DOI: 10.1038/nature14344]
- 23 **Galluzzi L**, Bravo-San Pedro JM, Kroemer G. Ferroptosis in p53-dependent oncosuppression and organismal homeostasis. *Cell Death Differ* 2015; **22**: 1237-1238 [PMID: 26143748 DOI: 10.1038/cdd.2015.54]
- 24 **Liu DS**, Duong CP, Haupt S, Montgomery KG, House CM, Azar WJ, Pearson HB, Fisher OM, Read M, Guerra GR, Haupt Y, Cullinane C, Wiman KG, Abrahmsen L, Phillips WA, Clemons NJ. Inhibiting the system x_c⁻/glutathione axis selectively targets cancers with mutant-p53 accumulation. *Nat Commun* 2017; **8**: 14844 [PMID: 28348409 DOI: 10.1038/ncomms14844]
- 25 **Hasegawa M**, Takahashi H, Rajabi H, Alam M, Suzuki Y, Yin L, Tagde A, Maeda T, Hiraki M, Sukhatme VP, Kufe D. Functional interactions of the cystine/glutamate antiporter, CD44v and MUC1-C oncoprotein in triple-negative breast cancer cells. *Oncotarget* 2016; **7**: 11756-11769 [PMID: 26930718 DOI: 10.18632/oncotarget.7598]
- 26 **Alvarez SW**, Sviderskiy VO, Terzi EM, Papagiannakopoulos T, Moreira AL, Adams S, Sabatini DM, Birsoy K, Possemato R. NFS1 undergoes positive selection in lung tumours and protects cells from ferroptosis. *Nature* 2017; **551**: 639-643 [PMID: 29168506 DOI: 10.1038/nature24637]
- 27 **Ritchie ME**, Phipson B, Wu D, Hu Y, Law CW, Shi W, Smyth GK. limma powers differential expression analyses for RNA-sequencing and microarray studies. *Nucleic Acids Res* 2015; **43**: e47 [PMID: 25605792 DOI: 10.1093/nar/gkv007]
- 28 **Doll S**, Freitas FP, Shah R, Aldrovandi M, da Silva MC, Ingold I, Goya Grocin A, Xavier da Silva TN, Panzilius E, Scheel CH, Mourão A, Buday K, Sato M, Wanninger J, Vignane T, Mohana V, Rehberg M, Flatley A, Schepers A, Kurz A, White D, Sauer M, Sattler M, Tate EW, Schmitz W, Schulze A, O'Donnell V, Proneth B, Popowicz GM, Pratt DA, Angeli JPF, Conrad M. FSP1 is a glutathione-independent ferroptosis suppressor. *Nature* 2019; **575**: 693-698 [PMID: 31634899 DOI: 10.1038/s41586-019-1707-0]
- 29 **Chen H**, Boutros PC. VennDiagram: a package for the generation of highly-customizable Venn and Euler diagrams in R. *BMC Bioinformatics* 2011; **12**: 35 [PMID: 21269502 DOI: 10.1186/1471-2105-12-35]
- 30 **Frost HR**, Amos CI. Gene set selection via LASSO penalized regression (SLPR). *Nucleic Acids Res* 2017; **45**: e114 [PMID: 28472344 DOI: 10.1093/nar/gkx291]
- 31 **Tang Z**, Kang B, Li C, Chen T, Zhang Z. GEPIA2: an enhanced web server for large-scale expression profiling and interactive analysis. *Nucleic Acids Res* 2019; **47**: W556-W560 [PMID: 31114875 DOI: 10.1093/nar/gkz430]
- 32 **Zhang Z**, Wang L, Wang Q, Zhang M, Wang B, Jiang K, Ye Y, Wang S, Shen Z. Molecular Characterization and Clinical Relevance of RNA Binding Proteins in Colorectal Cancer. *Front Genet* 2020; **11**: 580149 [PMID: 33193701 DOI: 10.3389/fgene.2020.580149]
- 33 **Liu J**, Huang X, Yang W, Li C, Li Z, Zhang C, Chen S, Wu G, Xie W, Wei C, Tian C, Huang L, Jeon F, Mo X, Tang W. Nomogram for predicting overall survival in stage II-III colorectal cancer. *Cancer Med* 2020; **9**: 2363-2371 [PMID: 32027098 DOI: 10.1002/cam4.2896]
- 34 **Fearnhead HO**, Vandenabeele P, Vanden Berghe T. How do we fit ferroptosis in the family of regulated cell death? *Cell Death Differ* 2017; **24**: 1991-1998 [PMID: 28984871 DOI: 10.1038/cdd.2017.149]
- 35 **Xie Y**, Zhu S, Song X, Sun X, Fan Y, Liu J, Zhong M, Yuan H, Zhang L, Billiar TR, Lotze MT, Zeh HJ 3rd, Kang R, Kroemer G, Tang D. The Tumor Suppressor p53 Limits Ferroptosis by Blocking DPP4 Activity. *Cell Rep* 2017; **20**: 1692-1704 [PMID: 28813679 DOI: 10.1016/j.celrep.2017.07.055]
- 36 **Malfa GA**, Tomasello B, Acquaviva R, Genovese C, La Mantia A, Cammarata FP, Ragusa M, Renis M, Di Giacomo C. *Betula etnensis* Raf. (Betulaceae) Extract Induced HO-1 Expression and Ferroptosis Cell Death in Human Colon Cancer Cells. *Int J Mol Sci* 2019; **20** [PMID: 31163602 DOI: 10.3390/ijms20112723]
- 37 **Li Y**, Chen W, Qi Y, Wang S, Li L, Li W, Xie T, Zhu H, Tang Z, Zhou M. H₂ S-Scavenged and Activated Iron Oxide-Hydroxide Nanospindles for MRI-Guided Photothermal Therapy and Ferroptosis in Colon Cancer. *Small* 2020; **16**: e2001356 [PMID: 32789963 DOI: 10.1002/smll.202001356]
- 38 **Wei G**, Sun J, Hou Z, Luan W, Wang S, Cui S, Cheng M, Liu Y. Novel antitumor compound optimized from natural saponin Albiziabioside A induced caspase-dependent apoptosis and ferroptosis as a p53 activator through the mitochondrial pathway. *Eur J Med Chem* 2018; **157**: 759-772 [PMID: 30142612 DOI: 10.1016/j.ejmech.2018.08.036]
- 39 **Gagliardi M**, Cotella D, Santoro C, Corà D, Barlev NA, Piacentini M, Corazzari M. Aldo-keto reductases protect metastatic melanoma from ER stress-independent ferroptosis. *Cell Death Dis* 2019; **10**: 902 [PMID: 31780644 DOI: 10.1038/s41419-019-2143-7]
- 40 **Chu B**, Kon N, Chen D, Li T, Liu T, Jiang L, Song S, Tavana O, Gu W. *ALOX12* is required for p53-mediated tumour suppression through a distinct ferroptosis pathway. *Nat Cell Biol* 2019; **21**: 579-591 [PMID: 30962574 DOI: 10.1038/s41556-019-0305-6]
- 41 **Holzner S**, Brenner S, Atanasov AG, Senfter D, Stadler S, Nguyen CH, Fristiohady A, Milovanovic D, Huttary N, Krieger S, Bago-Horvath Z, de Wever O, Tentes I, Özmen A, Jäger W, Dolznig H, Dirsch VM, Mader RM, Krenn L, Krupitza G. Intravasation of SW620 colon cancer cell spheroids

- through the blood endothelial barrier is inhibited by clinical drugs and flavonoids in vitro. *Food Chem Toxicol* 2018; **111**: 114-124 [PMID: 29129665 DOI: 10.1016/j.fct.2017.11.015]
- 42 **Resler AJ**, Makar KW, Heath L, Whitton J, Potter JD, Poole EM, Habermann N, Scherer D, Duggan D, Wang H, Lindor NM, Passarelli MN, Baron JA, Newcomb PA, Le Marchand L, Ulrich CM. Genetic variation in prostaglandin synthesis and related pathways, NSAID use and colorectal cancer risk in the Colon Cancer Family Registry. *Carcinogenesis* 2014; **35**: 2121-2126 [PMID: 24908683 DOI: 10.1093/carcin/bgu119]
- 43 **Liu S**, Yan B, Lai W, Chen L, Xiao D, Xi S, Jiang Y, Dong X, An J, Chen X, Cao Y, Tao Y. As a novel p53 direct target, bidirectional gene HspB2/ α B-crystallin regulates the ROS level and Warburg effect. *Biochim Biophys Acta* 2014; **1839**: 592-603 [PMID: 24859470 DOI: 10.1016/j.bbagr.2014.05.017]
- 44 **Li Q**, Wang Y, Lai Y, Xu P, Yang Z. HspB5 correlates with poor prognosis in colorectal cancer and prompts epithelial-mesenchymal transition through ERK signaling. *PLoS One* 2017; **12**: e0182588 [PMID: 28796798 DOI: 10.1371/journal.pone.0182588]
- 45 **Shi C**, Yang X, Bu X, Hou N, Chen P. Alpha B-crystallin promotes the invasion and metastasis of colorectal cancer via epithelial-mesenchymal transition. *Biochem Biophys Res Commun* 2017; **489**: 369-374 [PMID: 28506831 DOI: 10.1016/j.bbrc.2017.05.070]
- 46 **Weng ML**, Chen WK, Chen XY, Lu H, Sun ZR, Yu Q, Sun PF, Xu YJ, Zhu MM, Jiang N, Zhang J, Zhang JP, Song YL, Ma D, Zhang XP, Miao CH. Fasting inhibits aerobic glycolysis and proliferation in colorectal cancer via the Fdft1-mediated AKT/mTOR/HIF1 α pathway suppression. *Nat Commun* 2020; **11**: 1869 [PMID: 32313017 DOI: 10.1038/s41467-020-15795-8]
- 47 **Liu Y**, Guo F, Guo W, Wang Y, Song W, Fu T. Ferroptosis-related genes are potential prognostic molecular markers for patients with colorectal cancer. *Clin Exp Med* 2021 [PMID: 33674956 DOI: 10.1007/s10238-021-00697-w]
- 48 **Zhu L**, Yang F, Wang L, Dong L, Huang Z, Wang G, Chen G, Li Q. Identification the ferroptosis-related gene signature in patients with esophageal adenocarcinoma. *Cancer Cell Int* 2021; **21**: 124 [PMID: 33602233 DOI: 10.1186/s12935-021-01821-2]
- 49 **Zhuo S**, Chen Z, Yang Y, Zhang J, Tang J, Yang K. Clinical and Biological Significances of a Ferroptosis-Related Gene Signature in Glioma. *Front Oncol* 2020; **10**: 590861 [PMID: 33330074 DOI: 10.3389/fonc.2020.590861]
- 50 **Liang JY**, Wang DS, Lin HC, Chen XX, Yang H, Zheng Y, Li YH. A Novel Ferroptosis-related Gene Signature for Overall Survival Prediction in Patients with Hepatocellular Carcinoma. *Int J Biol Sci* 2020; **16**: 2430-2441 [PMID: 32760210 DOI: 10.7150/ijbs.45050]
- 51 **Dueland S**, Foss A, Solheim JM, Hagness M, Line PD. Survival following liver transplantation for liver-only colorectal metastases compared with hepatocellular carcinoma. *Br J Surg* 2018; **105**: 736-742 [PMID: 29532908 DOI: 10.1002/bjs.10769]
- 52 **Miao Y**, Li Q, Wang J, Quan W, Li C, Yang Y, Mi D. Prognostic implications of metabolism-associated gene signatures in colorectal cancer. *PeerJ* 2020; **8**: e9847 [PMID: 32953273 DOI: 10.7717/peerj.9847]
- 53 **Miao YD**, Wang JT, Yang Y, Ma XP, Mi DH. Identification of prognosis-associated immune genes and exploration of immune cell infiltration in colorectal cancer. *Biomark Med* 2020; **14**: 1353-1369 [PMID: 33064017 DOI: 10.2217/bmm-2020-0024]
- 54 **Rigo A**, Gottardi M, Zamò A, Mauri P, Bonifacio M, Krampera M, Damiani E, Pizzolo G, Vinante F. Macrophages may promote cancer growth via a GM-CSF/HB-EGF paracrine loop that is enhanced by CXCL12. *Mol Cancer* 2010; **9**: 273 [PMID: 20946648 DOI: 10.1186/1476-4598-9-273]
- 55 **Mizuno R**, Kawada K, Itatani Y, Ogawa R, Kiyasu Y, Sakai Y. The Role of Tumor-Associated Neutrophils in Colorectal Cancer. *Int J Mol Sci* 2019; **20** [PMID: 30691207 DOI: 10.3390/ijms20030529]
- 56 **Ruland J**. Colon Cancer: Epithelial Notch Signaling Recruits Neutrophils to Drive Metastasis. *Cancer Cell* 2019; **36**: 213-214 [PMID: 31526756 DOI: 10.1016/j.ccell.2019.08.010]
- 57 **Huang R**, Li Z, Zhu X, Yan P, Song D, Yin H, Hu P, Lin R, Wu S, Meng T, Zhang J, Huang Z. Collagen Type III Alpha 1 chain regulated by GATA-Binding Protein 6 affects Type II IFN response and propanoate metabolism in the recurrence of lower grade glioma. *J Cell Mol Med* 2020; **24**: 10803-10815 [PMID: 32757451 DOI: 10.1111/jcmm.15705]



Published by **Baishideng Publishing Group Inc**
7041 Koll Center Parkway, Suite 160, Pleasanton, CA 94566, USA
Telephone: +1-925-3991568
E-mail: bpgoffice@wjgnet.com
Help Desk: <https://www.f6publishing.com/helpdesk>
<https://www.wjgnet.com>

